NUST COLLEGE OF
ELECTRICAL AND MECHANICAL ENGINEERING

Design and Fabrication of a Pico Hydropower Generation System

A PROJECT REPORT

DE-41 (DME)

Submitted by

Ahsen Ali

Ahtasham Ahmed Virk

Abdussalam Majid

Muhammad Fouzan Butt

BACHELORS

IN

MECHANICAL ENGINEERING

YEAR

2023

PROJECT SUPERVISOR

Dr. Abdur Rehman Mazhar

NUST COLLEGE OF
ELECTRICAL AND MECHANICAL ENGINEERING
PESHAWAR ROAD, RAWALPINDI

DECLARATION

We hereby declare that no portion of the work referred to in this Project Thesis has been submitted in support of an application for another degree or qualification of this of any other university or other institute of learning. If any act of plagiarism is found, we are fully responsible for every disciplinary action taken against us depending upon the seriousness of the proven offence, even the cancellation of our degree.

COPYRIGHT STATEMENT

ACKNOWLEDGEMENTS

Firstly, we would like to thank almighty Allah for providing us with the strength and guidance to complete our final year project. Furthermore, we would like to express our sincerest gratitude to our supervisor, faculty, family members and colleagues. Their encouragement and assistance have played a crucial role in shaping the quality of our work. Lastly, we extend our heartfelt appreciation to all those who have directly or indirectly contributed to the successful completion of this thesis.

ABSTRACT

With an ever-increasing demand for energy and the depletion of naturally occurring resources, the focus is shifting towards devising clean and sustainable energy production methods. One of these methods is the usage of in-pipe hydropower generation systems in applications such as high-rise residential buildings, water transmission pipelines, and tropical areas where abundant rainfall is present. This system utilizes an in-pipe hydro turbine which uses the head and flowrate of water to produce mechanical energy which is then converted to electricity via a motor used in reverse as a generator. Initially, a thorough literature review was conducted and the Kaplan, Michell Banki, Darrieus and Savonius turbine were selected. Then, parameters such as efficiency, overall cost, Von Mises Stress, factor of safety (FOS) and what water heads and flowrates each turbine optimally operates in were considered and the Kaplan turbine was selected. Furthermore, the Kaplan turbine was designed according to our design parameters and a 3D CAD model was generated. Then, the turbine was 3D printed using Polyethylene Terephthalate Glycol (PETG) as the printing material due to its numerous advantages. Then, the in-pipe hydropower generation system was assembled and experimentally tested under the influence of various flowrates and parameters such as the voltage, current, rotational speed and power output were obtained. Lastly, the payback period was calculated across different flowrates for both domestic as well as industrial applications.

TABLE OF CONTENTS

Chapter 10

Conclusion

INTRODUCTION

1.1 Overview

As the overall population of the world increases, energy demand is on its peak. Furthermore, naturally occurring energy resources are depleting which have caused researchers to focus on finding new and innovative techniques to generate energy to reduce the gap between energy demand and supply. Therefore, the focus of energy production is shifting towards renewable energy systems such as energy harvesting. What is energy harvesting? Energy harvesting is the conversion of ambient energy present in the environment into electrical energy for use in powering autonomous electronic devices or circuits [1]. One of the methods of extracting energy and converting it into useful electrical energy which can be utilized for various applications such as domestic as well as industrial are hydroelectric power generation systems.

Next, what is the importance of hydroelectric power generation? Firstly, as stated by the United States Geology Survey (USGS) [2], hydroelectric power generation utilize the already present kinetic energy in the running water which makes it a renewable energy source. In addition, hydroelectric power generation systems can produce extensive amounts of energy in application which possess high water head via the abundant gravitational potential energy present in the water. Furthermore, as stated by Enel Green Power [3], hydroelectric power generation systems have high initial investment but become the cheapest energy source in the medium to long term. Next, hydroelectric power generation systems emit minute amounts of greenhouse gases (GHG) into the atmosphere. In addition, greenhouse gases (GHG) emitted by hydroelectric power generation systems are less compared to electric generation power plants operating on fossil fuels such as gas, coal and oil. Although only 33% of the hydroelectric potential is being utilized, hydroelectric power generation systems prevent the emissions of greenhouse gases (GHG) equivalent to the burning of 4.4 million barrels of petroleum worldwide daily. This results in a reduction of acid rain and smog which improves the Air Quality Index (AQI) of the surrounding air. Also, hydroelectric power generation systems do not produce any toxic by-products.

Furthermore, hydroelectric power generation systems possess the ability to reach from zero to maximum power production extremely quickly which makes them exceptionally appropriate to deal with any alteration in the consumption and providing ancillary services to the electricity system. Therefore, hydroelectric power generation systems provide stability, reliability and maintain the balance between electricity supply and demand [2]. Therefore,

hydroelectric power generation systems that are developed and operated in a manner that is economically viable, environmentally sensible and socially responsible represent the fundamental instrument for sustainable development.

LITERATURE REVIEW

Marco Casini [4] reviewed harvesting energy from in-pipe hydro systems. The review focused on the basics of hydropower systems. Firstly, the review paper stated that hydropower systems compose 16% of the overall electricity generation of the world and 85% of the overall renewable electricity generation of the world.

2.1 Categorization of In-Pipe Hydropower Systems

Category	**Power Production**
Large Hydro	Over 10 MW
Small Hydro	Up to 10 MW
Mini-Hydro	Up to 1MW
Micro-Hydro	Up to 100 KW
Pico-Hydro	Up to 5 KW

Category	**Basic Overview**
Internal	It is usually a Mini, Micro or a Pico hydro system which is composed of a turbine whose runner is present within the pipeline. Furthermore, only the generator is present outside the pipeline to convert the mechanical energy of the turbine into electrical energy. These systems are usually used for relatively smaller applications due to their compact size such as self-powered water monitoring systems.
External	It is usually a Mini, Micro, or a Pico hydro system composed of a generator and a turbine whose runner is present is a secondary channel that bypasses the main one. Therefore, a specified and larger casing is needed to accommodate the turbine and generator assembly. Due to this drawback, external in-pipe hydro systems cannot be directly applied to existing water piping systems.

2.2 Why are In-Pipe Hydro Systems preferred over Solar and Wind Energy?

Marco Casini [4] also reviewed the power, electric productivity and area required for installation for three different renewable systems. The three systems compared were Lucidpipe turbine, vertical axis Gorlov design wind turbine and monocrystalline silicon photovoltaic module. It was concluded that the productivity of the in-pipe hydro system was greater as compared to the other renewable energy systems. It was also observed that the productivity of the in-pipe hydro systems remained constant all year around. This was because in-pipe hydro systems are almost immune to climate changes such as wind speed and the intensity of solar radiation. The only parameter necessary to harness clean and safe energy from in-pipe hydro systems is that enough pressure is present within the water pipeline. Furthermore, in-pipe hydro systems require a relatively low area of installation. In addition, for these three renewable energy systems to produce the same amount of energy, wind energy renewable systems require four times the elements and forty times the area required for installation as compared to in-pipe hydro systems. Also, solar renewable energy systems require fifty-six times the elements and around ten times the area required for installation as compared to in-pipe hydro system. Therefore, these results show that the in-pipe hydropower systems possess a more stable productivity all year around and require a smaller area for installation which makes it feasible for harnessing clean and safe energy efficiently.

2.3 Applications of In-Pipe Hydropower Systems

2.3.1 In-Pipe Hydropower Systems in High-Rise Residential Buildings

Jiyun Du et al [5] analyzed the use of pump as turbine (PAT) in high-rise residential buildings. The study was conducted on a high-rise residential building in Hong Kong. The height was taken as the average of the residential buildings present in Hong Kong which was 26 storeys. Usually in high-rise residential buildings, the water pressure must be reduced to a proper value which ranges between ten to forty-five meters of water to minimize the risk of water leakages and the chances of water supply appliances to be damaged. The most utilized method of controlling the water pressure is by using pressure reduction valves in water pipelines. This is done by decreasing the available throttling area which in return increases the water head loss. In this research paper, pressure reduction valve is replaced by a pump which is used in reverse as a turbine in order to control the water pressure and generate electrical power simultaneously. Now, a question may arise as to why are typical micro-hydro turbines not used to control the water pressure and generate electrical output in high-rise residential buildings? The following table illustrates how micro-hydro turbines are classified [5].

Category	**Examples**
Impulse Turbines	Pelton, Turgo, Cross-flow
Reaction Turbines	Francis, Propeller, Kaplan

Next, to answer the previous question, the following table emphasizes and justifies on why a pump was used in reverse as a turbine for water pressure management and electrical power generation instead of typical micro-hydro turbines [5].

Micro-Hydro Turbine	**Justification**
Pelton, Turgo	It can be utilized at high or medium heads. It is usually installed in open environments with its runner not submerged in water. This makes these turbines unsuitable for water supply systems.
Cross-flow, Propeller	It can be utilized in water supply systems of high-rise buildings for electrical power generation but it has an unsatisfactory performance when it comes to water pressure management

Francis	It can be used it high-rise buildings for both water pressure management and electrical power generation. It has an efficiency ranging between 30% and 60% when applied to micro-sites. On the other hand, the overall cost in designing and manufacturing is relatively quite high which makes it unfeasible to use for economic reasons.

Pump as turbine (PAT) which basically means that a centrifugal pump is operated inversely to manage water pressure as well as generate electrical power output. Pump as turbine (PAT) is relatively cheap, easy to install and maintain and easiness to apply to different conditions due to its vast availability in the market. Furthermore, the efficiency of pump as turbine (PAT) can reach as high as 85%. In pump as turbine (PAT), its geometrical characteristics are fixed as well as its inner flow space, the water pressure management was extremely sensitive to the variation in the flow rate of water within the pipeline. On the other hand, pressure reduction valves can manage water pressure by adjusting the opening degree. Furthermore, in the research paper, the pump in turbine was selected using empirical formulas on which CFD analysis was carried out until the results obtained were satisfactory. Then, the selected pump as turbine (PAT) was utilized in the experimental setup. This process was carried until both the CFD analysis results and the experimental results agreed with each other. Two main design parameters on which the selection of the pump as turbine (PAT) depended upon were the flowrate of water within the water pipeline and the water head reduction. One of the main challenges in this research paper was to select the design flowrate of water within the pipeline as there was a fair amount of variation in the flowrate on an hourly basis. Then, the design flowrate of water within the pipeline was taken to be 10 m^3/h and the water head reduction ranged between thirty to thirty-five meters of water. The production of clean and safe energy was done in three steps. Firstly, hydropower was generated due to the flow of water. Then, hydropower was converted into the mechanical shaft power of the pump as turbine (PAT). Finally, mechanical power was converted into electricity with the help of a generator. These calculations were done using the equations shown in the following table [5].

Parameter	**Equation**
Theoretical Available Power	$P_{th} = \rho gHQ/3600$
Mechanical Shaft Power	$P_{me} = nT/9.55$
Actual Power Output	$P_{ac} = n_t n_{me} n_g \rho gHQ/3600$

Efficiency of Pump as turbine (PAT)	$n_t = P_{me}/P_{th}$

In this research paper, the pump as turbine (PAT) performance was theoretically calculated using the model proposed by Sun-Sheng Yang instead of other existing models due to its increased efficiency. The equations utilized for theoretical performance calculation are illustrated in the following table [5].

Equation Number	**Equation**
1	$Q_t/Q_p = 1.2/n_p^{0.55}$
2	$H_t/H_p = 1.2/n_p^{1.1}$

Furthermore, the standard k-ε and SST k-w models were utilized in the CFD analysis of the selected pump as turbine (PAT). Furthermore, to increase the efficiency of the CFD analysis, leakage was taken into consideration as a function of the geometry of the flow field and the head. The equations utilized to calculate the leakage are shown in the following table [5].

Parameter	**Equation**
Leakage Flow	$Q_L = (A_f + A_b)H_m^{0.5}$
Leakage Passage	$A = \frac{\pi\sqrt{2g}\mu\left(\frac{2cl}{D_s}\right)\left(\frac{\Delta H_{cl}}{H_m}\right)^{0.5}D_0^2}{2\left(\frac{D_0}{D_s}\right)^2\left(1-\left(\frac{D_h}{D_0}\right)^2\right)}$
Annular Fore Gap Diameter	$D_{sf} = 1.29D_0$
Annular Back Gap Diameter	$D_{sb} = 1.32D_0$
Head Reduction by Leakage	$H_L = \frac{3}{4}\frac{u_1^2 - u_2^2}{2g}$
Inlet Tangential Velocity	$u_1 = \frac{\pi D_1 N}{60}$
Outlet Tangential Velocity	$u_2 = \frac{\pi D_2 N}{60}$

Next, in the research paper, the results obtained from the computational analysis and experimental setup were compared. It was evident from the comparison that the SST k-w was

more accurate as compared to the standard k-ε model. Therefore, the CFD analysis results obtained from the SST k-w model were considered. The efficiency of the pump as turbine (PAT) used from the SST k-w model was obtained to be 19% while the efficiency obtained from the experimental setup was 11.5%. Furthermore, the best efficiency point of the selected pump as turbine (PAT) was at 1780 rpm. Another problem faced in this research paper was that when the flowrate of water in the pipeline exceeded the design flowrate, the water head reduction was greater than the design water heads reduction desirable range. On the other hand, when the flowrate of water in the pipeline was less than the design flowrate, the water head reduction lower than the desirable water head reduction range. Therefore, an installation and control strategy were utilized to keep the flowrate of the water within the pipeline near the design flowrate and the water head reduction within the acceptable range. This was done by installing the pump as turbine (PAT) in parallel with motorized control valve which catered for both flowrates below the design flowrate as well as flowrates above it. Due to this, even for flowrates greater than the design flowrate, the water head reduction stabilized at thirty-three meters of water. After applying the installation and control strategy, the maximum electrical power output at the design flowrate of 10 m^3/h was around 100 W with a water head reduction of thirty-three meters.

Furthermore, Prabir Sarkar et al [6] analyzed energy generation potential from grey water in high-rise building in Mumbai, India. In this study, a twenty-story building was taken into consideration with an average of 100 residents on each floor. Furthermore, it was assumed that the water consumption per resident was 171 L. In this study, a water collection tank is placed on the 10^{th} floor which collects grey water from all the floors above it. Therefore, the water in the collection tank possesses potential head (stored energy). Once an abundant amount of grey water is collected, the water level sensor opens the valve at the bottom of the pipe connected to the tank. Then, the water flows downward within the pipeline and strikes the blades of the Pelton turbine. Thus, the turbine shaft rotates and produces mechanical energy which is converted to electrical energy via a generator. This electrical energy can be either utilized on the spot or stored within batteries for later use. It was concluded that the total energy output in this system was around 6.8525 KWh. Furthermore, a 1:30 scaled down experimental setup was installed on campus which verified that the collection tank must be placed at a minimum height of 10 floors in order to harness reasonable safe and clean energy. Finally, the cost benefit analysis of the system installed in the twenty-story building was done. It was concluded that it had a payback period of around 8 years.

2.3.2 Hydro-Turbines in Water Transmission Pipelines

Youssef Itani et al [7] analyzed recovering energy in a water transmission pipeline in Saudi Arabia with the use of hydro-turbines. The main objective of this research paper was to decrease CO_2 emission by harnessing clean and safe electrical power output from the flowrate of the water within the pipeline. The differences between the two groups of turbines known as reaction and impulse are illustrated in the table below [7].

Turbine Group	**Turbines**	**Difference**
Reaction	Kaplan, Propeller, Francis and Pump as turbine (PAT)	These turbines are designed for low water head systems. Furthermore, Francis turbines and Pump as turbines (PATs) can manage higher heads relative to Kaplan turbines. The major drawback is that the efficiency of these turbines decreases when a low flow condition exists.
Impulse	Pelton, Turgo and Cross-flow	These turbines are not utilized in applications in which downstream pressure is required. In addition, impulse turbines are more costly relative to reaction turbines.However, an advantage of impulse turbines is that its efficiency does notvary with changing flowrates of water within the pipeline.

This research paper has also stated the developments which have been made in the field of hydro-turbines with the aim of decreasing the overall CO_2 emissions by harnessing clean and safe energy. A few of these developments are illustrated in the following table [7].

Study Number	**Results and Observations**
1	Christine Power et al [8] analyzed the method of harvesting energy in wastewater treatment plants with the use of hydropower turbines at the discharge points. In this study, the

	key factors were taken to be flowrate of water within the pipeline, selection of turbine, financial incentives and electricity prices. Furthermore, the turbines under consideration were Kaplan, Francis, Propeller and pump as turbine (PAT). It was concluded that the electrical power output varied between the range of 3 KW to 234 KW depending on the different discharge flowrates and available heads at the selected wastewater treatment plants in the UK and Ireland. Due to different discharge flowrates and available heads, the payback period varied from approximately 3 years to 24 years. Also, it was also observed that the difference in discharge flowrates due to demographic and climate conditions directly affected the overall efficiency of the hydro-turbine as well as its selection.
2	Eva Gomez-L1anos et al [9] utilized MATLAB to identify the potential spaces in which Pico hydro-turbines could be installed in a 200 mm pipeline. The Pico hydro-electric powerplant was manufactured using ductile cast iron which has an absolute roughness (K) of approximately 0.2 mm. Furthermore, the pipe in consideration had a length of 1000 m and efficiency of the turbine was 80 %. It was concluded that electrical power output obtained a maximum value of 87 KW. The flowrate within the pipeline varied from 0.01 m^3/s to 1 m^3/s while the head varied between the range of 10 m to 120 m.
3	Asmae Berrada et al [10] utilized an optimization algorithm obtain the maximum overall efficiency in installing micro hydropower turbines in water systems in Morocco. In this proposed model, the hydro-plant components are optimized by maximizing the energy production through the optimization of the net head. In addition, the ideal head is reached when the hydropower plant's pipe diameter is properly sized to minimize pressure losses. Furthermore, it was concluded that by optimizing the hydropower plant, the pressure losses present significantly decreased while the energy output increased. It

	was also observed that by varying the capacity factor of the hydropower plant, the economic benefits ranged from 900,000 to 1,800,000 Euros. Finally, after the optimization of the hydropower plant with a capacity factor of 80%, the electrical power output was 69 KW and the overall CO_2 emissions decreased by 282 tons.
4	Min Liu et al [11] developed a theoretical model for the energy performance of the pump as turbine (PAT) as well as in pump mode. For the theoretical model of pump mode, numerous factors such as theoretical head, loss in inlet pipe, loss in impeller which includes surface friction loss, blade loading loss, separation loss, wake mixing loss, recirculation loss, disk friction loss and leakage loss, loss in volute, friction loss of spiral and diffuser part and pump efficiency were taken into consideration. Furthermore, for the theoretical model of the pump used inversely as a turbine, numerous factors such as theoretical head, loss in volute, loss in impeller which includes incidence loss, surface friction loss, blade loading loss, disk friction loss and leakage loss, loss in outlet pipe and turbine efficiency were taken into consideration. This aids in determining the best efficiency point. Furthermore, it was concluded the best efficiency point of pump operated inversely as a turbine is slightly lower than when it is operated in the pump mode.
5	Roland Uhunmwangho et al [12] analyzed the performance of mini hydro- turbines in Bumaji stream in Nigeria. The analysis was done in the rainy season which meant that the flowrate of water in the stream was maximum. In this study, the turbines in consideration were Kaplan, Francis, Turgo and Cross-flow turbines. It was observed that Kaplan turbine had the highest peak efficiency value of 0.9 at a range of 60% - 100% rated river flow. Furthermore, it also had the highest peak power output of 748 W. Also, Francis turbine had a peak efficiency of

	0.88 at a range of 80% - 100% rated river flow with a peak power output of 700 W. Turgo turbine had a peak efficiency value of 0.85 at a range of 40% - 100% rated river flow with a peak power output of 710 W. Furthermore, Cross-flow turbine had the lowest peak efficiency of 0.79 at a range of 90% - 100% rated river flow with the lowest power output of 670 W. It was concluded that the Cross-flow turbines generated the cheapest electrical power at 100.8 $/MWh, yearly saving 63,000 $, and having a payback period which was less than 5 years. Furthermore, the Kaplan turbine generated electricity at 106.2 $/MWh, yearly saving 52,000 $ and having a payback period of 5 years.

In this research paper, a water pipeline of 230 km and made of Carbon steel grade (X65) with a diameter of 40". Furthermore, this water pipeline transmits water from a main reservoir located 1790 meters above the ground. Firstly, by using WaterCAD simulation, the locations were determined which possessed residual pressure. These locations were termed as hotspots at which the appropriate hydropower turbine was to be installed. In addition, 8 hotspots were determined within the water pipeline. As usual, pressure reduction valves and flow control valves were utilized before water was discharged into the water tank at each hotspot. The equation used to calculate the embedded power at each hotspot is illustrated in the following table [7].

Parameter	**Equation**
Power Generated by Turbines	$P = ng\rho QH_{net}$

Then, MATLAB analysis was carried out for four different scenarios with variation in the velocity of the water in the pipeline from less than 1 m/s to a maximum value of 2.5 m/s to determine the most suitable scenario for the reduction in CO_2 emissions by harnessing clean and safe energy. The equations utilized in the simulations of different scenarios are presented in the following table [7].

Parameter	**Equation**
Friction Losses in Each Part of the System	**Hazen-Williams Equations**

	$h_f(\mathrm{m}) = 10.67\ L\ (\frac{AxV}{C})^{1.852}\ D^{-4.87}$
Calculated Pump Head	$H_p = Z_d - Z_p + \sum_0^n h_f$

Therefore, the residual pressure at each hotspot for each of the four scenarios were calculated. Next, MATLAB software was utilized in order to determine the most suitable turbine. The selection criteria were between Francis, Kaplan and Pelton turbine. When the parameters such as electro-mechanical cost and the electrical power output were taken into consideration, the Pelton turbine was selected. It was also visible from the efficiency curves of these turbines that the Pelton turbine was the most appropriate choice as its efficiency did not vary with fluctuations in the flowrate within the water pipeline. Furthermore, a turbine selections chart developed by Penche and Minas was also taken into consideration for the turbine selection. Next, economic factors such as the electro-mechanical cost and the energy payback period was calculated using the equations as shown in the table below [7].

Parameter	**Equation**
Electro-Mechanical Cost Pelton: Francis: Kaplan:	$17{,}693\ P^{-0.3644725}\ H^{-0.281735}$ $25{,}698\ P^{-0.560135}\ H^{-0.127243}$ $33{,}236\ P^{-0.58338}\ H^{-0.113901}$
Energy Payback Period	PP = Total Installation Cost/Annual Revenue

After analyzing the four different scenarios of flow velocity within the pipeline, scenario 3 was selected in which the velocity ranges from 1.5 m/s to 2 m/s. This selection was done based on economic factors, electric power output and the reduction in the CO_2 emissions. It was concluded that scenario 3 had an energy payback period of around 9.5 years. Furthermore, the average electro-mechanical cost taken over the eight hotspots was almost 267 €/KW and the overall electrical power output generated was around 5750 KW. Another factorcatered in this review paper was the observation of the yearly CO_2 emissions with and withoutthe installation of the hydropower turbines. It was observed that the difference in the CO_2 emissions with and without the installation of hydropower turbines was 35,295 tons yearly.

Furthermore, Teruhisa Kumano [13] et al analyzed the installation of micro in-pipe hydropower plant at a university building. Firstly, a scaled down prototype of the system was

manufactured and its results were observed. The scaled down system was composed of hydro turbine rotors, water guides and fan blades. In this study, the in-pipe micro hydropower generation system was assumed to be installed at the bottom of the drainage pipes. This allowed the maximum exploitation of the available flowrate of water within the pipeline and the net head. One of the advantages of this micro hydropower generation system was that energy production was also available during power outages if water was present in the above storage tank. Furthermore, the electrical output from the generator was connected to the ac system via a PWM inverter to help regulate output power appropriately. One of the issues of this micro hydropower generation system was that there was a small amount of water leakage from the system. It was concluded from the scaled down prototype of the system that the minimum energy output of 5 mW was achieved with an efficiency of 25.5% when four blades were utilized with a flowrate of 20 cc/sec within the pipeline. Furthermore, the maximum energy output of 44 mW was achieved with a maximum efficiency of 39.6% when six blades were utilized with a flowrate of 22.7 cc/sec within the pipeline. Next, in the research paper, this micro hydropower generation system was installed in a university building of 11 stories. It was observed that an electrical output of 91 W was generated. Finally, it was also concluded that an electrical output of 375 W was generated during heavy rainfall season.

2.3.3 Lift -Based In-Pipe Hydro-Turbine in Water Distribution Networks

Temidayo Lekan Oladosu et al [14] performed the numerical analysis of a lift-based in-pipe hydro turbine to predict the potential of harnessing clean and safe energy as well as optimize the water distribution network. The research paper gave reference on a recent study performed by installing a five blades tubular propeller turbine in a water pipeline. The results obtained are presented in the following table [14].

Study Number	**Results and Observations**
1	Irene Samora et al [15] analyzed experimental characterization of a five-blade tubular propeller turbine for pipe inline installation. The five-blade propeller turbine was operated at rotational speeds between the range of 750 rpm to 1000 rpm and flowrates within the pipeline ranging from 15 m^3/h to 25 m^3/h for maximum efficiency. It was concluded that the efficiency of the installation of the five blades tubular propeller

	turbine was around 64 % when it was operated at its best efficiency point. At the best efficiency point, the flowrate of the water within the pipeline was 16 m^3/h, rotation speed of 750 rpm and water head of 3.5 m. Furthermore, the maximum mechanical power output was around 330 W. At this condition, the flowrate of the water within the pipeline was 48 m^3/h, rotation speed of 1500 rpm and a water head of 4.9 m.

In this research paper, three public universities (University of Ibadan, Ibadan (UI), Obafemi Awolowo University Ile-Ife (OAU), and the Federal University of Technology Akure (FUTA)) were selected in southwestern Nigeria. Furthermore, the volumetric discharge rates of each of these universities were taken on hourly basis for the whole day. It was the main objective of the research paper to estimate the power potential of harnessing clean and safe energy as well as optimize the water distribution system of these three public universities selected. As emphasized in previous research papers in the previous sections, the parameters selected for the optimization of the water distribution systems of these three public universities selected were the discharge flowrates within the pipeline and the available effective water head available. Furthermore, a lift-based spherical turbine was selected for the numerical analysis as it minimizes cavitation and maximizes the conversion of axial energy to rotating energy. The basic parameters of the lift-based spherical turbine are illustrated in the following table [14].

Parameter	**Selected Value**
Turbine Diameter	0.2336 m
Turbine Height	0.1988 m
Chord Length	0.0287 m
Hub Diameter	0.1000 m
Turbine Shaft Diameter	0.0100 m
Blockage Ratio	0.1100 m
Number of Blades	4
Equatorial Solidity	0.1800 m
Average Solidity	0.2200 m

Next, the material of the lift-based spherical turbine was selected. Stainless Steel 304 was selected due to its global recommendation by the World Health Organization as it is nonhazardous when it meets edible substances. In addition, Aluminum 6061 was also selected due its light weight as well as its compounds significance in municipal water treatment. Next,

empirical formulas were utilized to calculate significant parameters which are shown in the following table [14].

Parameter	**Equation**
Blade Solidity	$\text{Blade Solidity} = c/s$ $s = 2\pi r_m/Z_b,\ r_m$
Tip Speed Ratio	$\lambda = (\omega * r)/v$
Hydrofoil Cross-Sectional Profile	$y_t = 5tc\left[0.2969\sqrt{\frac{x}{c}} + (-0.1620)(x/c) + (-0.3516)(x/c)^2 + 0.2843(x/c)^3 + (-0.1015)(x/c)^4\right]$
Time Steps Calculation	$T = D/(N * 6)$
Simulated Mechanical Power	$P_m = T_s * \omega_s$

Furthermore, the mass moment of inertia of the turbine made from the two selected materials was calculated for the water pipelines having a diameter of 100 mm and 250 mm respectively. Also, the numerical analysis was done for both the maximum and the minimum flowrate of water within the water distribution system of the three selected public universities. The obtained results for the lift-based spherical turbine manufactured from stainless steel 304 are illustrated in the following table [14].

University	**Pipeline Diameter**	**Maximum and Minimum Flowrates**	**Power Output**
OAU	250 mm	281 m^3/h	985.05 W
		163 m^3/h	437.72 W
UI	250 mm	323 m^3/h	1079.55 W
		230 m^3/h	944.60 W
		140 m^3/h	299.14 W
		112 m^3/h	242.25 W
FUTA	100 mm	288 m^3/h	8.10 W
		72 m^3/h	1.96 W

The obtained results for the lift-based spherical turbine manufactured from Aluminum 6061 are illustrated in the following table [14].

University	**Pipeline Diameter**	**Maximum and Minimum Flowrates**	**Power Output**
OAU	250 mm	281 m^3/h	1294.94 W
		163 m^3/h	897.91 W
UI	250 mm	323 m^3/h	1663.26 W
		230 m^3/h	1128.22 W
		140 m^3/h	669.46 W
		112 m^3/h	415.70 W
FUTA	100 mm	288 m^3/h	9.92 W
		72 m^3/h	4.89 W

Finally, it was observed in this paper that the percentage head loss within the water distribution system having a diameter of 250 mm possessed a loss less than 10% of the effective head available. Also, it was also concluded that the water distribution system having a diameter of 100 mm possessed high head loss.

2.3.4 Banki Inline Turbine for Pressure Regulation and Energy Production

Marco Singara [16] analyzed the backpressure Banki inline turbine for both pressure regulation as well as energy production. Banki/Cross-flow turbines are relatively small as compared to pump as turbine (PAT) and their axis is always orthogonal to the pipe direction. Therefore, the direction of flow within the pipeline is always present in the vertical plane including the pipe axis. Furthermore, a simple mobile flap can control the size of the inlet impeller surface. This aids in applications where constant flowrates within the pipeline and variable net head are present as it allows for the change in the characteristic curve with a small decline in the overall efficiency. As stated in the research paper, the traditional Banki/Cross-Flow turbines which were designed to be utilized in applications in which free outlet conditions were present had low overall efficiency. However, with the advancement in the designcriterion, the efficiency of the Banki/Cross-flow turbine has reached 90%. Furthermore, PRS Banki/Cross-flow turbines which can be applied in applications which have positive outflow pressure have a hydraulic efficiency of 70%. The PRS Banki/Cross-flow turbine can be

utilized in both the active and passive mode. The differences between these two modes are present in the following table [16].

Mode	**Working Principle**
Active	1. Provides discharge regulation by fixing the outlet piezometric level corresponding to the required discharge. 2. Transforming the inlet-outlet hydraulic power difference into electricity. 3. Pressure metering
Passive	1. Sets the outlet piezometric level at any required value, lower than the inlet one, but even much greater than the ground elevation, while also being variable in time. 2. Transforming the inlet-outlet hydraulic power difference into electricity. 3. Measuring the flowrate within the pipeline.

Next, the turbine was designed using empirical formulas which are presented in the following table [16].

Parameter	**Equation**
Inlet Velocity	$V = C_V \sqrt{2g\left(\Delta H - \xi \frac{\omega^2 D^2}{8g}\right)}$ $\frac{0.85\omega D}{\cos \alpha} = V$
Flowrate	$Q = \frac{BD\lambda_{rmax} V \sin \alpha}{2}$

Furthermore, CFD and experimental analysis were carried out on the PRS Banki/Cross-Flow turbine. In the experimental analysis, the PRS Banki/Cross-Flow turbine prototype was observed under the conditions where the flowrate varied from 5.9 l/s to 30 l/s and the flap position ranged from 30^0 to 90^0 of the impeller inlet angle. It was observed that PRS

Banki/Cross-Flow turbine at the best efficiency point (BEP) achieved an efficiency of 76.3% and a net head of 26.5 m at a discharge flowrate of 29.5 l/s, impeller inlet angle of 90^0 and a velocity ratio of 1.7. On the other hand, the minimum turbine efficiency was observed to be 30 % at a discharge flowrate of 5.3 l/s. When the results from the CFD and the experimental analysis were compared, the error present was 1.5%. It was also concluded that when a PRS Banki/Cross-Flow turbine and a pump as turbine (PAT) with similar characteristic curve were utilized under the same conditions, the energy output of the Banki/Cross-Flow turbine was greater than the pump as turbine (PAT) as it could cater for the variation in the flowrate of water within the pipeline.

In addition, Yang Hongxing [17] analyzed a method to enhance the performance of an inline Cross-Flow hydro turbine for power supply to water leakage monitoring system. Cross-Flow turbines are given preference when hydropower energy is harvested. This is due to its simple construction, low cost and wide working flow range. However, when Cross-Flow turbines are utilized in hydropower systems, the water flow exerts negative torque on the returning blades which decreases the overall efficiency of the Cross-Flow turbine. Previous studies have placed ducted/augmented elements surrounding the impeller to increase flow velocity, pressure difference and shield the flow towards the returning blades. In this research paper, two blocks are located on the upstream side and the downstream side of the impeller. The geometrical factors of the blocks taken into consideration are listed in the following table [17].

Geometric Factors	**What It Determines?**	**Selected Value**
Inlet Charge Angle (δ)	Magnitude of inlet velocity	120^0
Attack Angle (α)	Flow inlet direction	22^0

Next, in the research paper, CFD analysis was done using the SST k-w model. The tip speed ratio (TSR) was taken into consideration and its equation is shown in the following table [17].

Parameter	**Equation**
Tip Speed Ratio (TSR)	$TSR = \frac{r\omega}{V}$

It was observed that the upstream and downstream blocks acted as a nozzle and a diffuser respectively. Due to placing the blocks, the pressure difference between the upstream and the downstream side increases which results in more water passing through the Cross-Flow turbine. It was concluded that the maximum energy output of the Cross-Flow turbine was 136 W when the tip speed ratio (TSR) was 1.2. Furthermore, water head loss occurred in the range of 3.45 m to 3.75 m which had a negligible negative impact on the normal water supply.

MATHEMATICAL MODEL

3.1 TURBINE SELECTION

3.1.1 Kaplan Turbine

Kaplan turbines are axial flow turbines in which the water flows through the runner along the direction parallel to the axis of rotation of the runner [18]. It consists of four main components which are scroll casing, guide vane mechanism, draft tube and runner blades. In Kaplan turbines, water within the pipeline coming from an overhead reservoir enters the scroll casing which is specifically designed in such a way so that the flow pressure is not lost. Next, the water is directed to the runner blades via guide vanes which possess the ability to adjust themselves depending on the flowrate of water within the pipeline. The water makes a 90^0 turn, aligning its direction with that of the runner blades. Furthermore, the runner blades are twisted throughout their length to always ensure an optimum angle of attack throughout the overall cross section of the blades. This results in an increase in the overall efficiency of the Kaplan turbine. Also, the runner blades revolve because of the water's reaction force. Then, water enters the draft tube from the runner blades where both its kinetic and pressure energy are reduced. Kaplan turbines are usually installed in applications which possess low net head and high flowrates which range from 1.5 to 20 m and 3 m^3/s to 30 m^3/s respectively [19]. Lastly, Kaplan turbines produce high shaft speeds at low heads with efficiency in the range of 90 to 93 % which makes them extremely suitable for small-scale hydropower plants [20].

3.1.2 Banki-Michell Turbine

Banki-Michell turbines are impulse turbines made up of two main components: runner/wheel and nozzle. Water within the pipeline coming from an overhead reservoir is guided towards the impeller which is housed in a specifically designed rectangular sectioned production chamber. In addition, the duct segment may be partially divided by a distributor in accordance with the actual discharge value. Furthermore, the impeller is designed to resemble an empty wheel and is made up of two circular plates connected by several blades. Next, the jet is directed towards the center of the wheel before returning to cross additional blades before exiting [21]. Therefore, a narrow jet of water travels twice through the runner from the nozzle before being discharged. Banki-Michell turbines are usually installed in applications which possess both low water head and flowrates. Furthermore, the efficiency of Banki-Michell turbines ranges between 70 to 85 % which is almost invariable with respect to changes in the flowrate of water within the pipeline [22].

3.1.3 Darrieus Turbine

Darrieus turbines are wind turbines with long, thin loop-shaped blades linked to the top and bottom of the axle [23]. Even though Darrieus turbines are efficient, a few critical problems, such as torque ripple and cyclic pressures on the tower, cause early damage to its parts and joints. Additionally, the turbine's poor self-starting capabilities necessitates the use of an external power source or an additional Savonius rotor to start it. Furthermore, H-Darrieus/ straight-bladed and Gorlov rotor/helical bladed Darrieus hydro kinetic turbines are preferred due to their design simplicity and high efficiency in hydro energy harvesting applications. Next, due to pressure and shear distributions, hydrodynamic forces are generated on the hydrofoil surface as water within the pipeline coming from an overhead reservoir with a velocity v encounters the streamlined rotor blades at an angle of attack α. These hydrodynamic forces can be divided into two force components which are lift force F_L and drag force F_D. In addition, in Darrieus turbines, the pressure difference on a hydrofoil's surface primarily generates the lift force F_L, which is regarded as the primary force behind the generation of torque and power. On the other hand, the drag force F_D is negligible compared to the lift force F_L.

3.1.4 Savonius Turbine

Savonius turbine’s rotor’s basic form is a ‘S’ shape with a short overlap between its two semicircular blades [24]. In addition, Savonius turbines are inexpensive, have a straightforward design and produce low levels of noise. With good starting characteristics, Savonius turbines can receive fluid from any direction. Furthermore, Savonius turbines consist of two vertical half cylinders known as the advancing blade and the returning blade. Due to difference of drag force F_D between the concave and the convex parts of the rotor blades, a pair of couple forces are generated which rotate the semicircular blades which in return generates torque and power. In addition, deflectors are utilized to increase the overall coefficient of performance ofSavonius turbines. Lastly, Savonius hydrokinetic turbines can be installed in applications in which water within the pipeline coming from an overhead reservoir possesses low speeds in the range of 0.5 m/s and greater.

3.2 TURBINE DESIGN

3.2.1 Kaplan Turbine

Given Parameters:

1) Pipe Diameter = 4 in = 0.1016 m

2) Gross Head = 11 m

Design Parameters [25]:

Specific Speed $N_S = \frac{885.5}{H^{0.25}} = \frac{885.5}{(11m)^{0.25}} = 486.2$

$\Phi = 0.0242 N_S^{2/3} = 0.0242(486.2)^{2/3} = 1.496^0$

Turbine Speed $N = \frac{(84.5)*(\Phi)*(\sqrt{H})}{D_{Runner}} = \frac{(84.5)*(1.496^0)*(\sqrt{11m})}{0.1016m} = 4126.6$ rpm

Power $P = (\frac{(N_s)*(H^{\frac{5}{4}})}{N})^2 = (\frac{(486.2)*(11m)^{\frac{5}{4}}}{4126.6\ rpm})^2 = 5.57$ KW

Discharge $Q = \frac{(P)*(1000)}{(n)*(\rho g H)} = \frac{(5.57KW)*(1000)}{(0.9)*(1000\frac{kg}{m^3})*(9.81\frac{m}{s^2})*(11m)} = 0.05735\ m^3/s$

Diameter of Hub $D_{Hub} = m*(D_{Runner}) = (0.4)*(0.1016\ m) = 0.04064$ m

Flow Area $= \frac{\pi(D_{Runner}^2 - D_{Hub}^2)}{4} = \frac{\pi((0.01016m)^2 - (0.04064m)^2}{4} = 6.81 \times 10^{-3}\ m^2 = 68.1\ cm^2$

Flow Velocity $V_f = \frac{Q}{Flow\ Area} = \frac{0.05735\frac{m^3}{s}}{6.81*10^{-3}\ m^2} = 8.42$ m/s

Average Diameter $D_{avg} = \frac{D_{Runner} + D_{Hub}}{2} = \frac{(0.1016m)+(0.04064m)}{2} = 0.07112$ m

Average Velocity $V_{avg} = \frac{\pi(D_{avg})^2*(N)}{60} = \frac{\pi(0.07112)^2*(4126.6rpm)}{60} = 15.37$ m/s

Whirl Velocity $V_\omega = \frac{(P)*(1000)}{(\rho Q V_{avg})} = \frac{(5.57KW)*(1000)}{(1000\frac{kg}{m^3})*(0.05735\frac{m^3}{s})*(15.37\frac{m}{s})} = 6.32$ m/s

Next, by utilizing the design parameters, the coordinates of the selected airfoil NACA 4412 already present online [26] were translated according to our design criteria to provide us with five sections of the Kaplan turbine blade via a MATLAB code [27]. Then, the data was imported into SolidWorks and the 3D CAD model of the Kaplan turbine was generated.

MATLAB Code [27]:

```
clc
clear all

%Inputs
P = input('Power Output (KW) \n'); %Power Output in KW
H = input('Head Available (m) \n'); %Head Available in m
eff = input('Overall Efficiency \n'); %Overall Efficiency
Z = input('Number of Blades \n'); %Number of Blades
attack = input('Optimum Angle of Attack (deg) \n'); %Optimum Angle of Attack

density = 1000;
bladesections = 5; %For Design

%Discharge
Q = P.*1000./(eff.*density.*9.81.*H);
%Specific Speed
Ns = 885.5./(H.^0.25);
%Turbine Speed
N = Ns.*(H.^1.25)./(P.^0.5);
phi = 0.0242.*(Ns.^(2./3));

d_runner = 84.5.*phi.*(H.^0.5)./(N);
m = 0.4; %m = d_hub/d_runner
d_hub = m.*d_runner;

flowarea = pi.*((d_runner.^2)-(d_hub.^2))./4;
%Flow Velocity
V_f = Q./flowarea;
%Whirl Velocity
d_avg = (d_runner + d_hub)./2;
V_avg = pi.*d_avg.*N./(60);
V_w = P.*1000./(density.*Q.*V_avg);

s = linspace(1.3,0.75,bladesections);
i = 1;

for d = linspace(d_hub,d_runner,bladesections)
    U = (pi.*d.*N)./60;
    beta_1 = atand(V_f./(U-V_w));
    beta_2 = atand(V_f./U);

    %Blade  Spacing;
    t  =  (pi.*d)./Z;
    chord = s(i).*t;
    theta = 180 -beta_1 + attack;
    [naca] = xlsread('naca.xlsx');
    x = naca(:,1);
    y = naca(:,2);
    x = x*chord;
    y = y*chord;
    x = x - (chord/2);
    R = [cosd(theta) sind(theta); -sind(theta) cosd(theta)];
    rot_matrix = R*[x';y'];
    X_cord = rot_matrix(1,:)';
    Y_cord = rot_matrix(2,:)';
    Z_cord = zeros(35,1);
    X_cord = round(X_cord,6);
```

```
    Y_cord = round(Y_cord,6);
    figure
    plot(X_cord,Y_cord);
    set(gcf,'position',[0,0,800,800])
    section = [X_cord Y_cord Z_cord];
    writematrix(section,['section' num2str(i) '.txt'],'delimiter','tab')
    i = i+1;
end
```

Input:

```
Power Output (KW)
5.57
Head Available (m)
11
Overall Efficiency
0.9
Number of Blades
6
Optimum Angle of Attack (deg)
5
```

Output:

Section 1

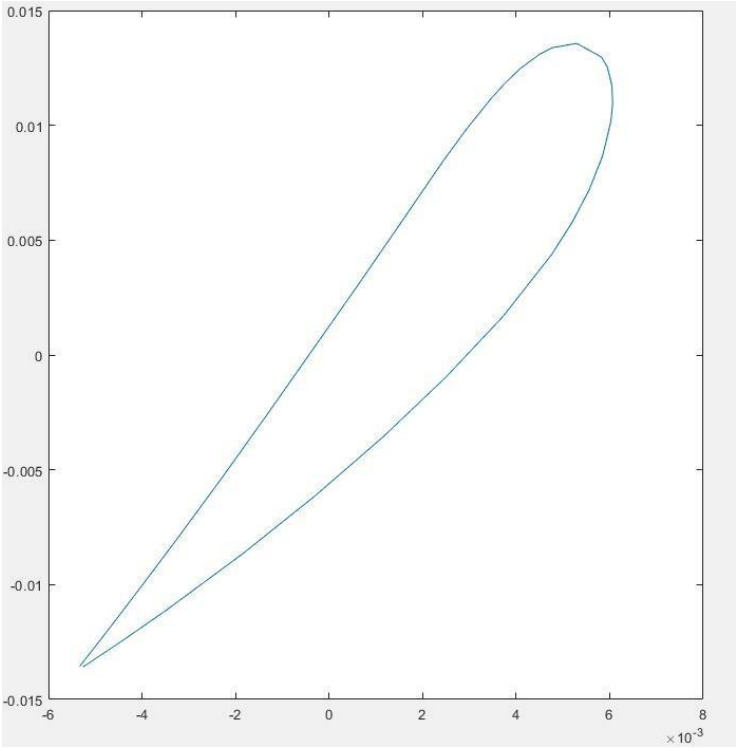

Section 2

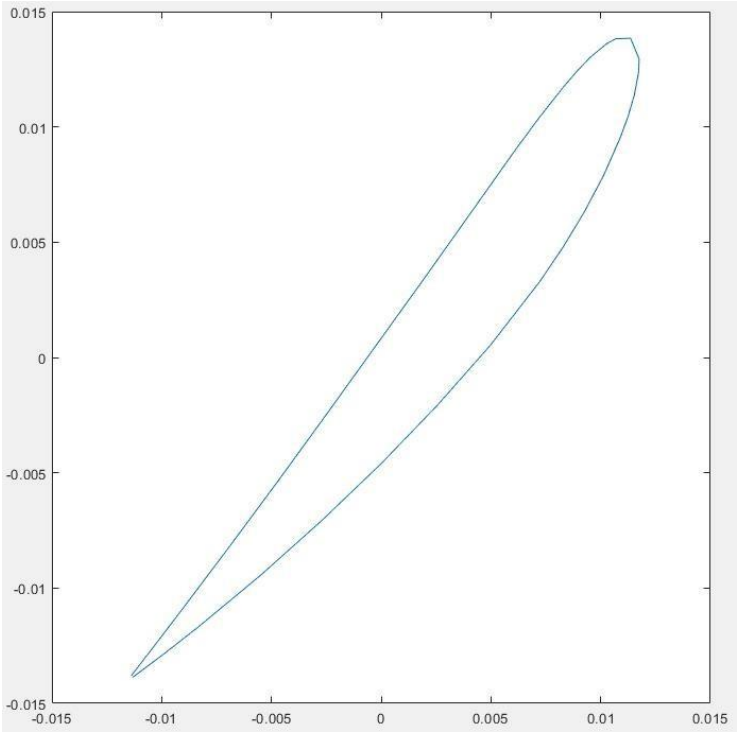

Section 3

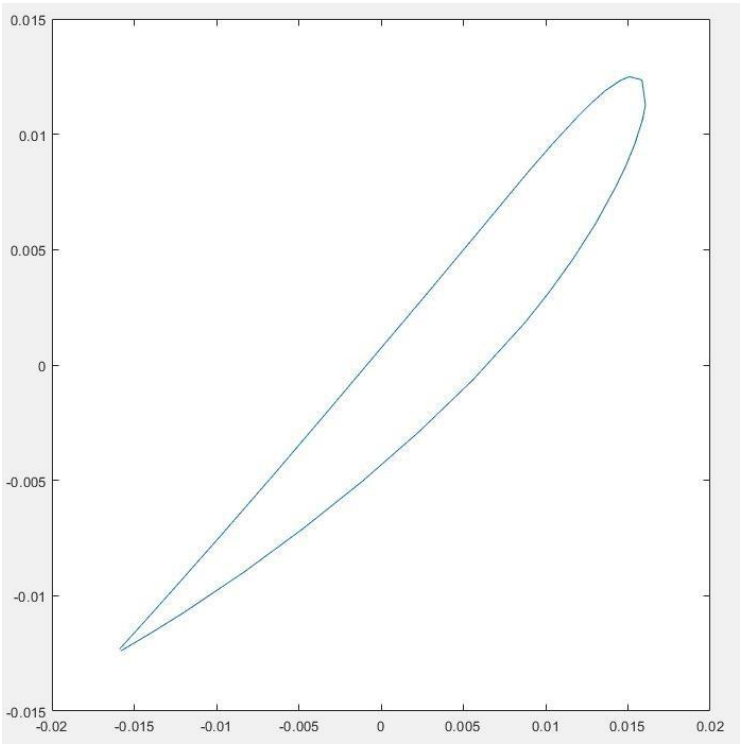

Section 4

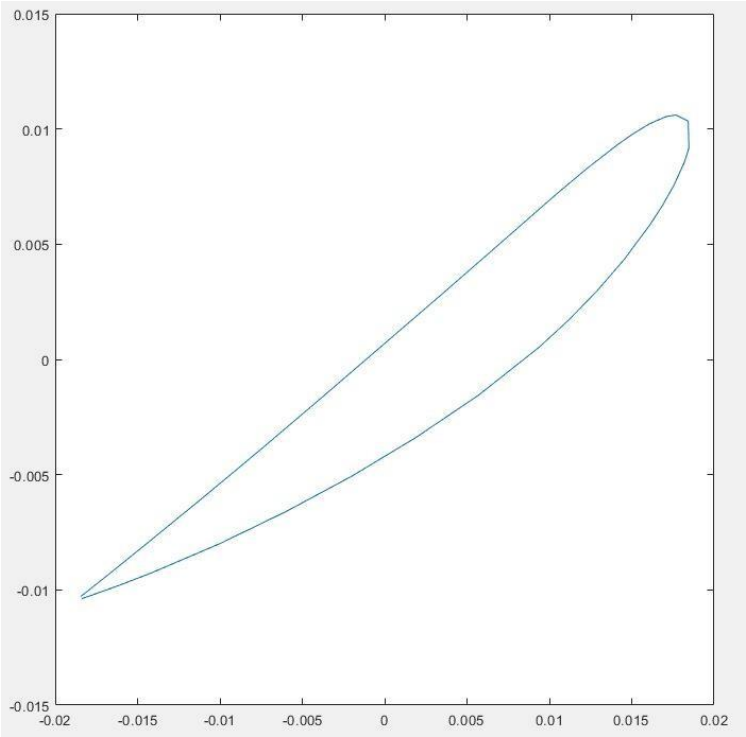

Section 5

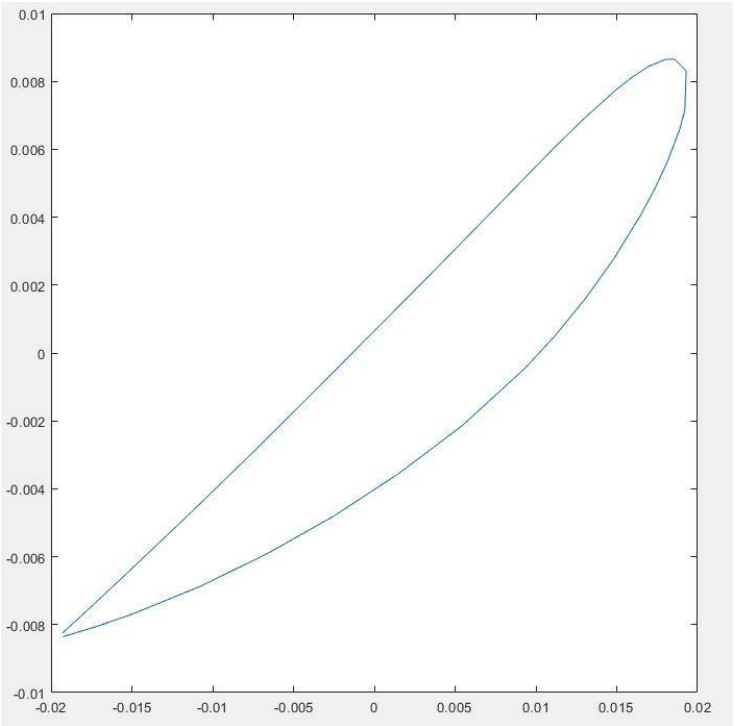

3D CAD Model

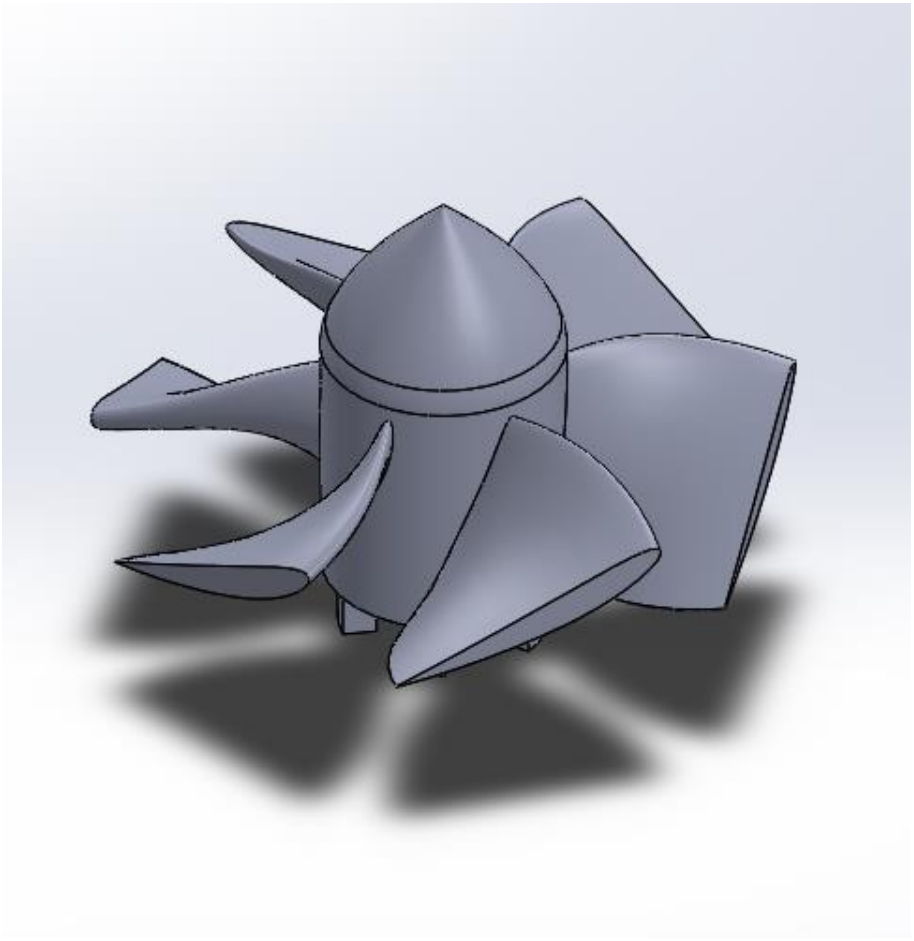

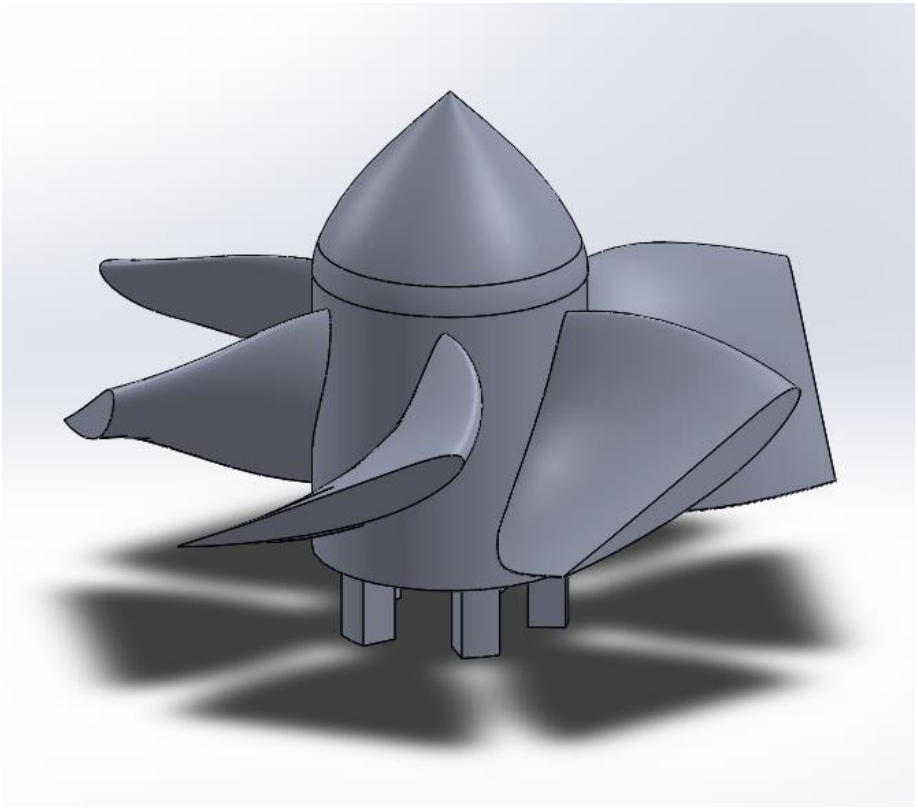

3.2.2 Banki Michell Turbine

Given Parameters:

1) Pipe Diameter = 4 in = 0.1016 m

2) Gross Head = 11 m

3) Design Flowrate = 0.05735 m^3/s

Design Parameters [28][29]:

Angle of Attack $\alpha = 22^0$

Inlet Flow Angle $\beta_1 = 2*(\tan(\alpha)) = 2*(\tan(22^0)) = 39^0$

Outlet Flow Angle $\beta_2 = 90^0$

Nozzle Entry Arc Angle $\lambda = 90^0$

Efficiency n = 0.80 or 80 %

Real Rotational Speed N_{real} = 757 rpm

Characteristic Speed N_s = 95.78

Dimensionless Rotational Speed N^* = 540.714

Dimensionless Flowrate Q^* = 0.00004

Unit Rotational Speed N^1 = 574.82 rpm

In [29], the Banki Michell turbine was integrated into a system which utilized a DN250 pipe and a DN 100 T-joint. Furthermore, there are no empirical formulas to relate the pipe diameter to the T-joint diameter. Therefore, the ratios of pipe diameter to T-joint diameter were equated to obtain the outer diameter D_1 of the Banki Michell turbine according to our design criteria.

$$\frac{0.106\text{m}}{\substack{T-Joint \\ Diameter}} = \frac{0.25m}{0.1m}$$

$$\text{T-Joint Diameter} = \frac{(0.1016m)(0.1m)}{0.25m} = 0.04064 \text{ m} = 40.64 \text{ mm}$$

Therefore, we have selected the T-Joint diameter to be 40 mm with respect to product reference manuals from manufacturers.

A tolerance of 2 mm was selected in our design criteria to ensure that the Banki Michell turbine could be inserted into the pipeline.

Outer Diameter D_1 = 0.038 m = 38 mm

Inner Diameter D_2 = 0.68*(D_1) = 0.68*(0.038m) = 0.02584 m = 28.84 mm

Curvature Radius $\rho_b = \frac{[0.019m^2 - 0.01292m^2]}{2[(0.019m)(cos39^0)+(0.01292m)(cos90^0)]}$ = 6.57 x 10^{-3} m

Angle at Centre of Blade $\delta = 2*\tan^{-1}\frac{[cos39^0 - \frac{0.019m}{0.01292m}cos90^0]}{[sin39^0 - \frac{0.01292m}{0.019m}sin90^0]} = 61.4^0$

In [29], figure 10 illustrates the relation between efficiency vs number of blades. It can be concluded that maximum efficiency can be obtained when the number of blades of the Banki Michell turbine N_b = 35.

Furthermore, Table 3 illustrates the blade thickness t_b obtained from various design parameters in multiple studies. Since there are no empirical formulas to obtain the blade thickness t_b, a reasonable blade thickness t_b has been selected based on the data available within the table according to our design criteria.

t_b = 2.5 mm

3D CAD Model

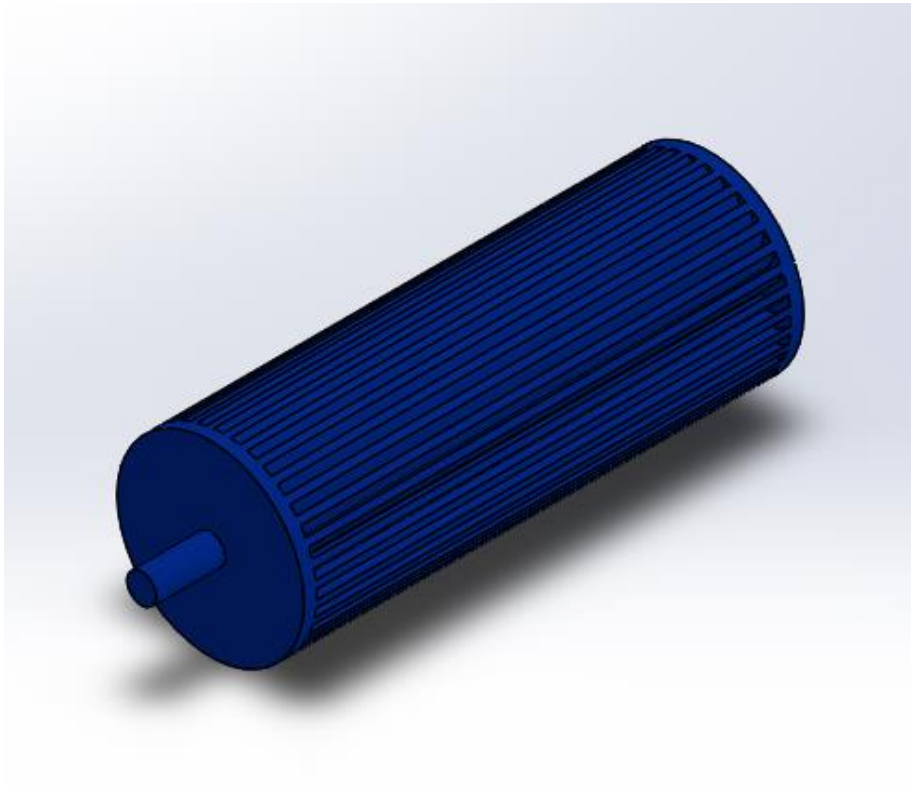

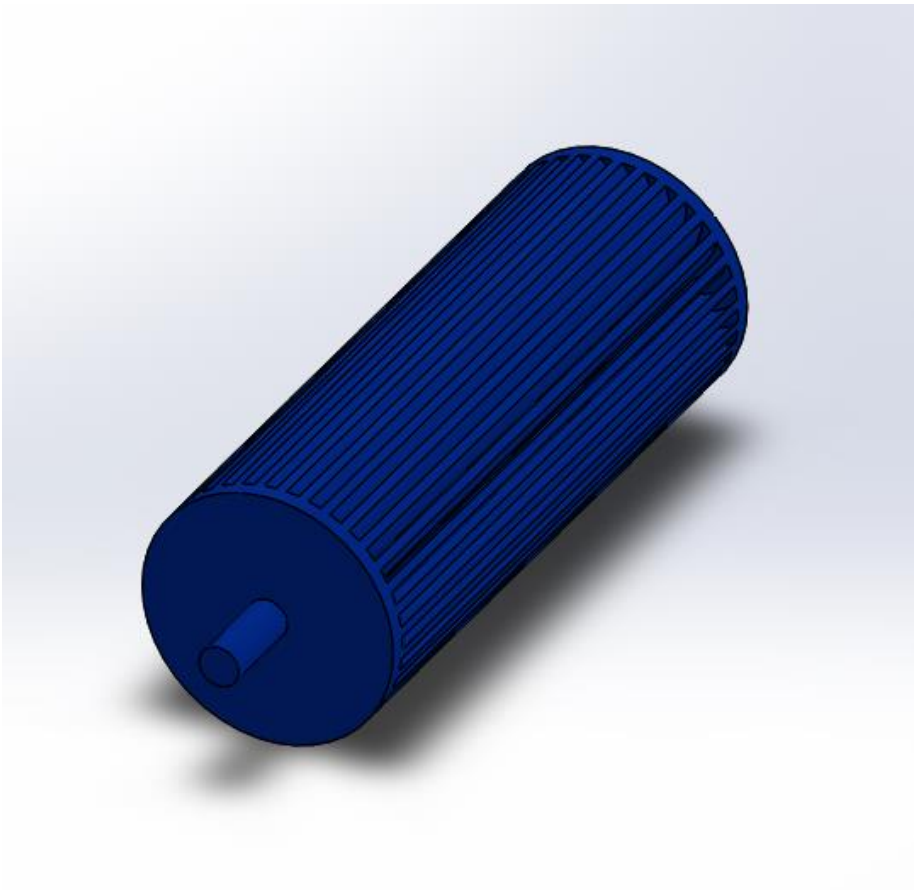

3.2.3 Darrieus Turbine

Given Parameters:

1) Pipe Diameter = 4 in = 0.1016 m

2) Gross Head = 11 m

3) Design Flowrate = 0.05735 m^3/s

Design Parameters [30]:

Airfoil used: NACA 0020

Diameter of The Turbine = 0.1016 m = 101.6 mm

Solidity $\sigma = 0.382$

Blade number n = 6

Helical Angle $\varphi = 60^0$

Height of The Turbine $H = \frac{\tan(60^0)*(\pi)*(0.1016m)}{6}$ = 0.0921 m = 92.1 mm

Aspect Ratio $AR = \frac{H}{D} = \frac{0.1016m}{0.0921m}$ = 0.906

Enwinding Ratio $\varpi = 1.25$

Blade Projection Angle $\psi = \frac{(360)*(\varpi)}{n} = \frac{(360)*(1.25)}{6} = 75^0$

Chord Length $C = \frac{(\sigma)*(D)*(\pi)}{n} = \frac{(0.382)*(0.1016m)*(\pi)}{6}$ = 0.02032 m = 20.32 mm

3D CAD Model

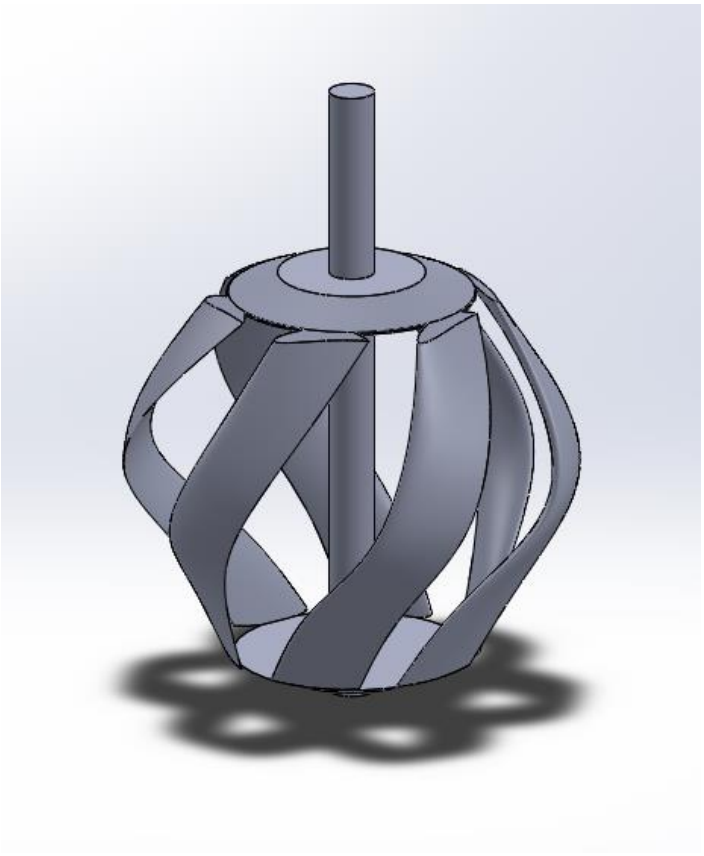

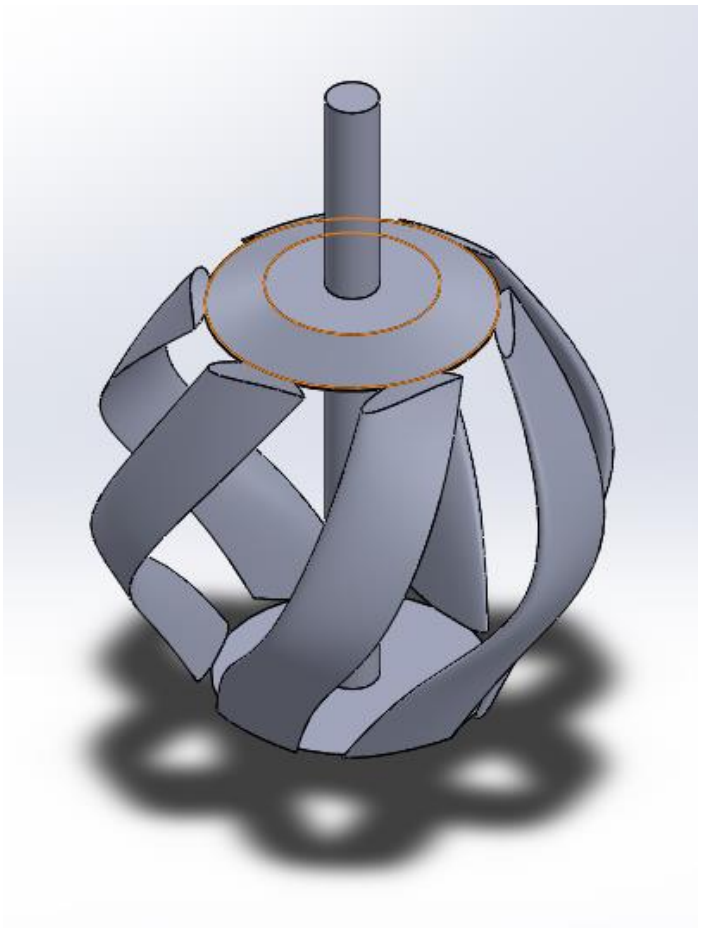

3.2.4 Savonius Turbine

Given Parameters:

1) Pipe Diameter = 4 in = 0.1016 m

2) Gross Head = 11 m

3) Design Flowrate = 0.05735 m^3/s

Design Parameters [31]:

Pipe Diameter D_0 = 0.01016 m = 101.6 mm

Clearance ε = 4 mm

Biggest Turbine Diameter D = (101.6 mm) – 2(4 mm) = 93.6 mm

Aspect Ratio AR = 0.9

Height of The Turbine H = (AR)*(D) = (0.9)*(93.6 mm) = 84.24 mm

Maximum Turbine Blade Angle $\theta_{max} = \sin^{-1}(AR) = \sin^{-1}(0.9) = 64.2^0$

Thickness of The Blade t_b = 2 mm

Local Semi-Circle Diameter d_i = 65.52 mm

Overlap Ratio = 0.20 or 20 %

Initial Overlap e = (Overlap Ratio)*(D) = (0.20)*(93.6 mm) = 18.72 mm

Secondary Overlap $e' = 0$

Deflector Angle $\alpha = 80^0$

Blockage Coefficient = 0.8

3D CAD Model

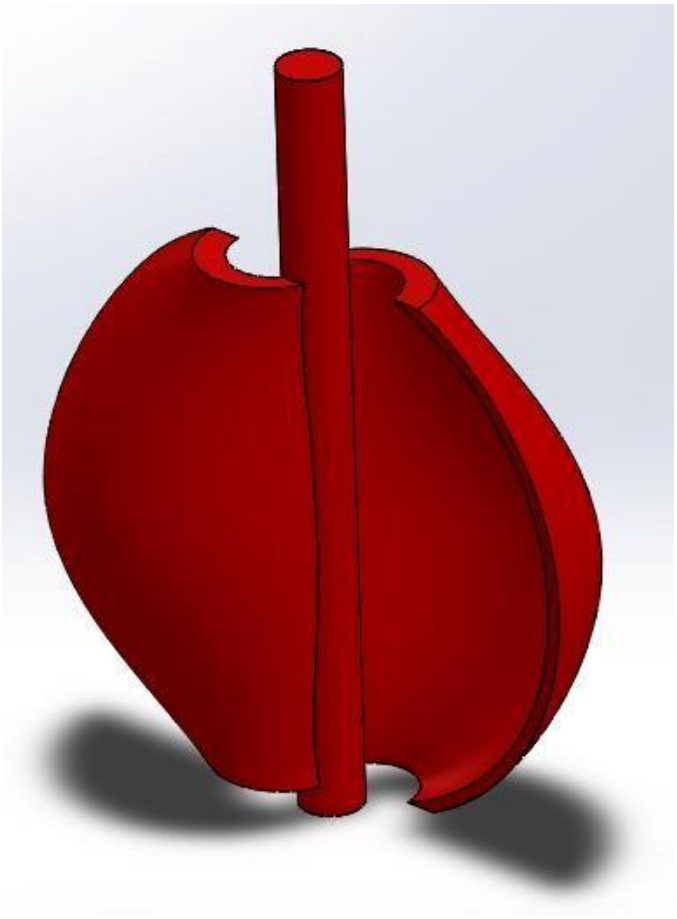

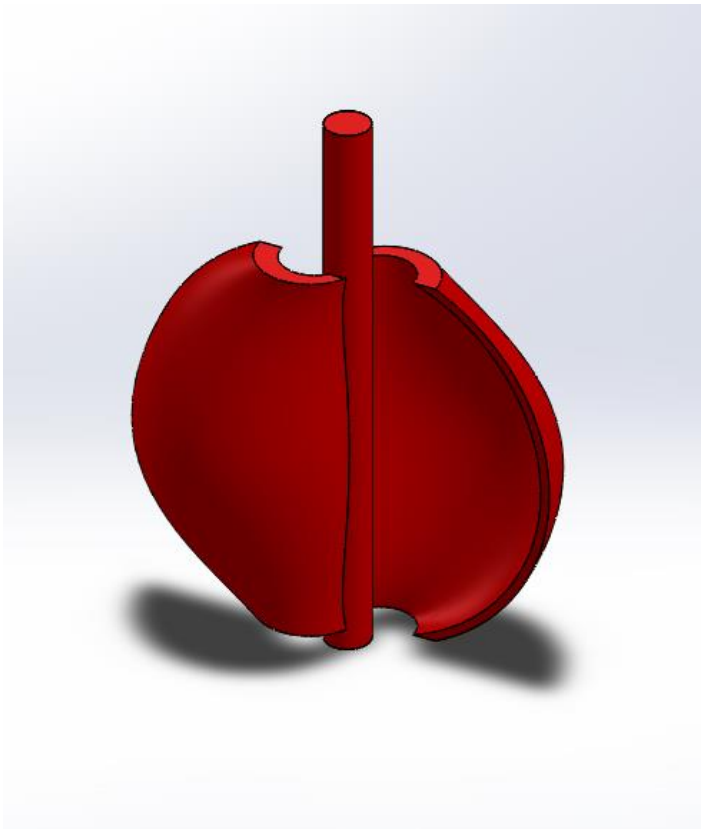

SIMULATIONS

4.1 Overview

Firstly, the 3D model of the Kaplan, Banki Michell, Darrieus and Savonius turbines were constructed using SOLIDWORKS. Then, ANSYS workbench was utilized to perform ANSYS CFX and Structural analysis of the selected turbines. The main goal of the simulations was to obtain the Von Mises stress as well as the factor of safety (FOS) of each turbine under a design flowrate of 1 Kg/s. Finally, multiple parameters such as overall cost, suitable applications, efficiency ranges and the factor of safety (FOS) were considered in selecting the most suitable turbine for fabrication.

4.2 Procedure

Firstly, the 3D model of the turbine was imported into ANSYS CFX and was generated. Next, delete commands were utilized to remove the excess geometry. Then, using the extrude command, a fluid domain was created around the turbine. Furthermore, a Boolean command was utilized to subtract the turbine from the fluid domain and the resulting wireframe was obtained.

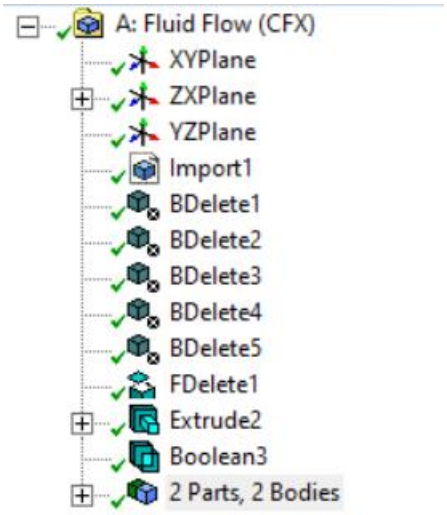

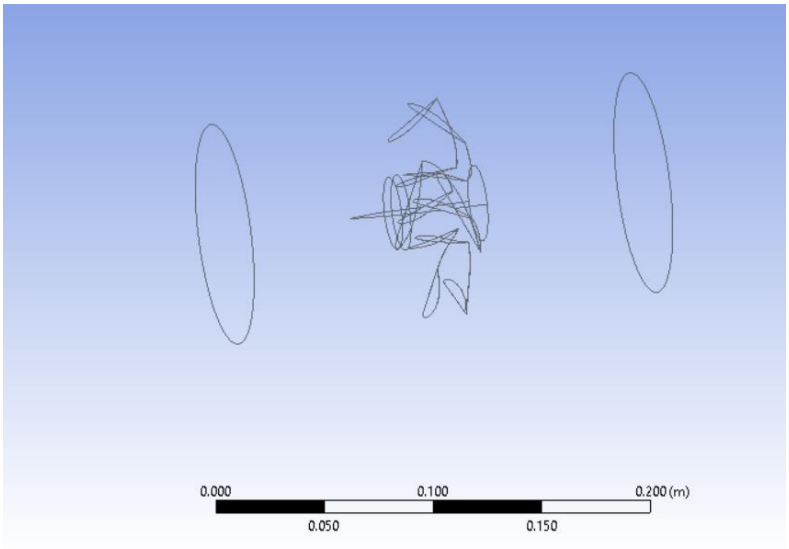

Furthermore, the inlet, outlet, wall and turbine were created as named sections. Next, the properties of the mesh were set to have a linear element as well as high smoothing in order to obtain more accurate results. Then, the mesh was generated.

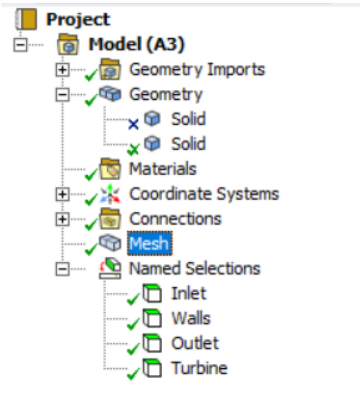

Element Order	Linear
Element Size	2.0 mm
Sizing	
Quality	
Check Mesh Qua...	Yes, Errors
Target Skewn...	Default (0.9)
Smoothing	High
Mesh Metric	None
Inflation	
Advanced	
Statistics	
Nodes	118755
Elements	622374

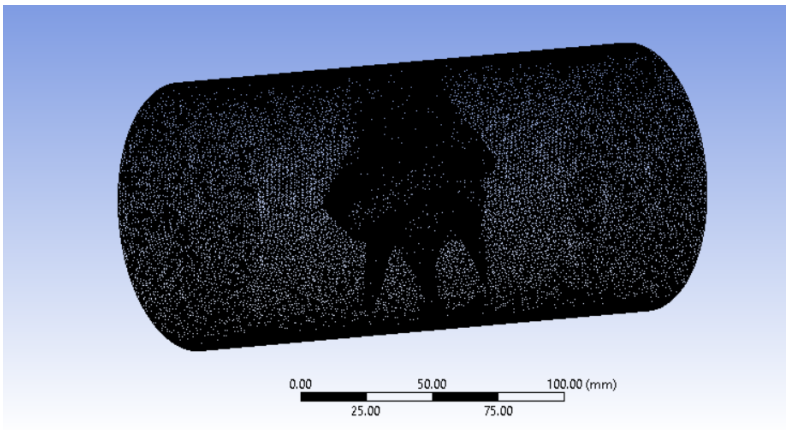

Next, the fluid was defined as water and the analysis was defined as steady state. Then, the inlet velocity was set as 7 m/s. In this case, since it is a steady state analysis, the outlet velocity does not vary and remains constant as 7 m/s.

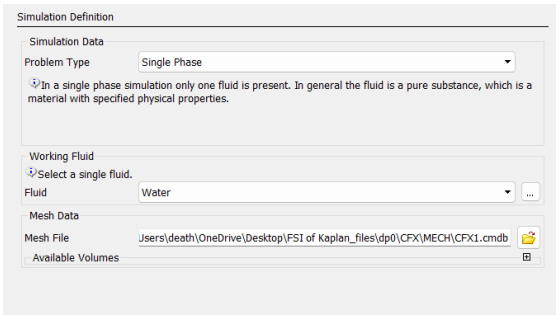

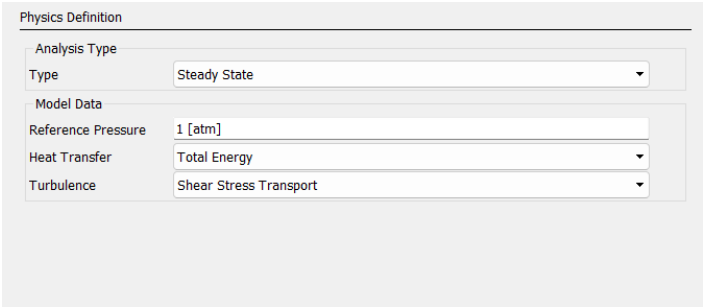

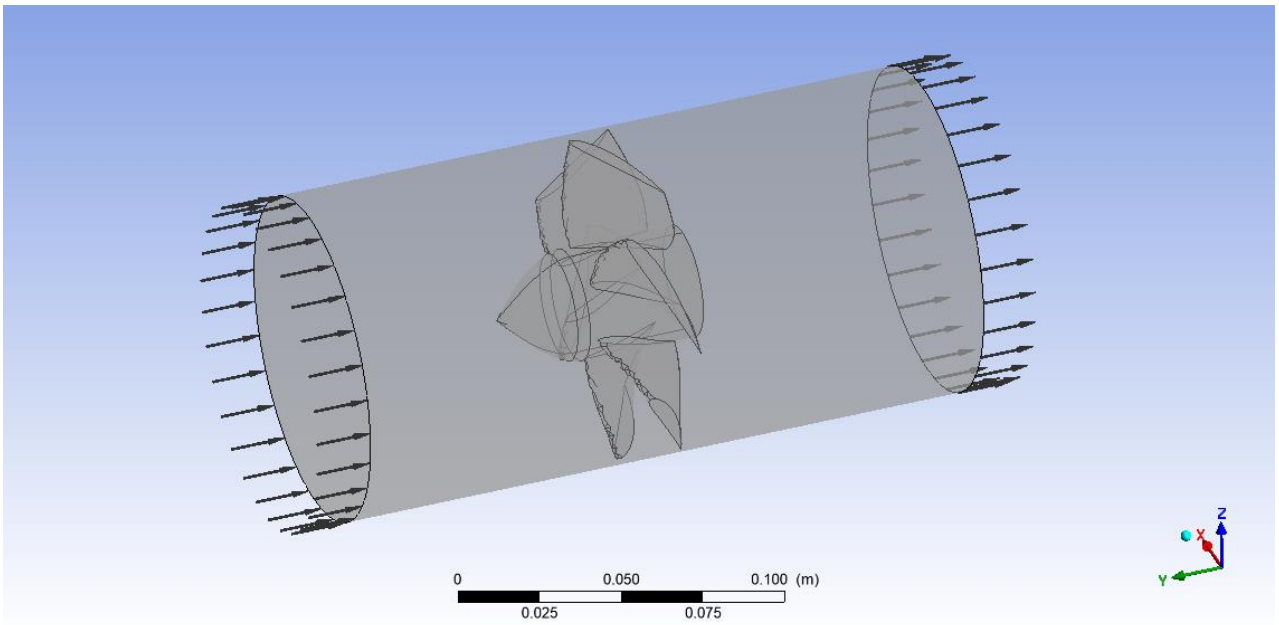

Then, the solution of ANSYS CFX was calculated. The convergence criteria was kept as default and the solution converged in only 49 iterations.

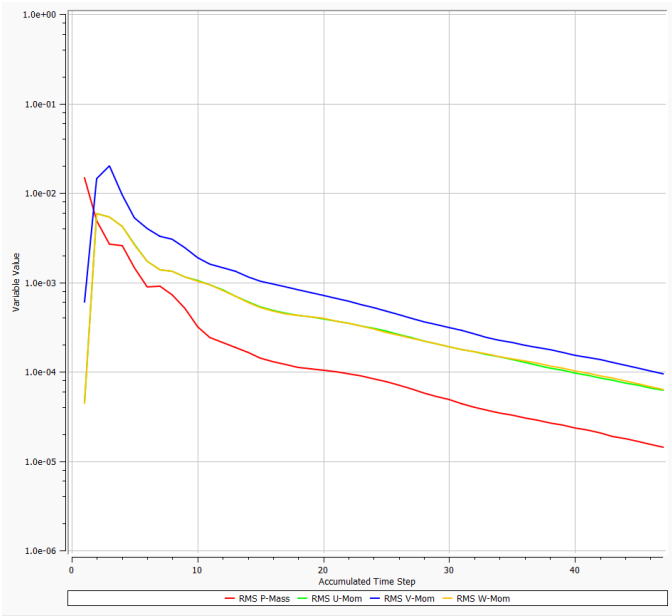

Then, the solution of ANSYS CFX was made to be the input for the ANSYS Static Structural analysis. Next, the mesh properties were set to have high smoothing in order to obtain accurate results. Then, the mesh was generated.

Details of "Mesh"

Element Size	1.0 mm
Sizing	
Quality	
Check Mesh Quality	Yes, Errors
Error Limits	Aggressive Mechanical
Target Element Quality	Default (5.e-002)
Smoothing	High
Mesh Metric	None
Inflation	
Advanced	
Statistics	
Nodes	407176
Elements	268576

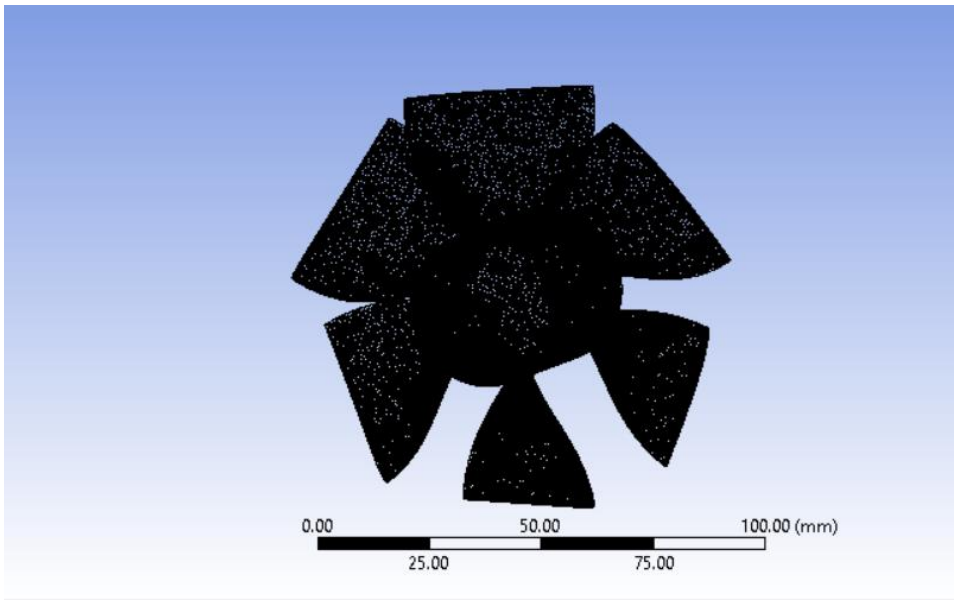

As stated earlier, the parameters of interest were the Von Mises stress and the factor of safety (FOS) of each turbine under the design flowrate of 0.05735 m^3/s. Furthermore, the above-mentioned procedure was carried out for the Kaplan, Banki Michell, Darrieus and Savonius turbines individually. Finally, the solution was obtained.

4.3 Von Mises and FOS Contours

4.3.1 Kaplan Turbine

Von Mises Contour

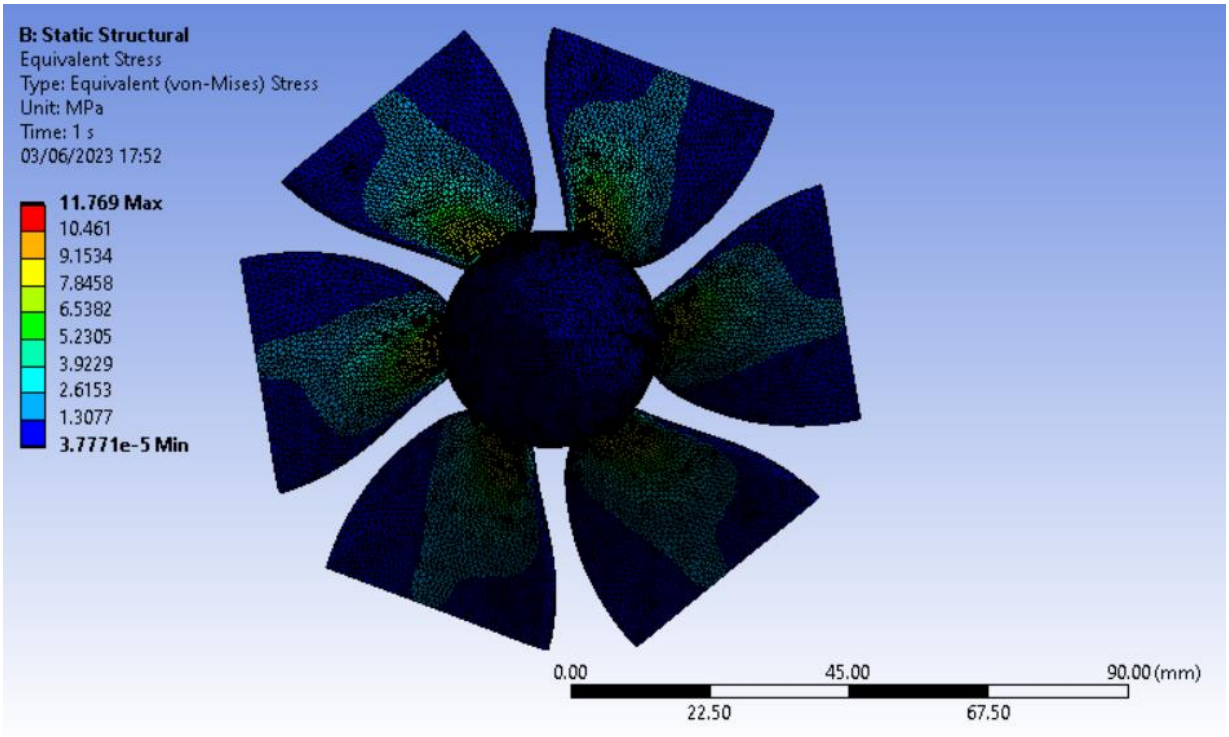

FOS Contour

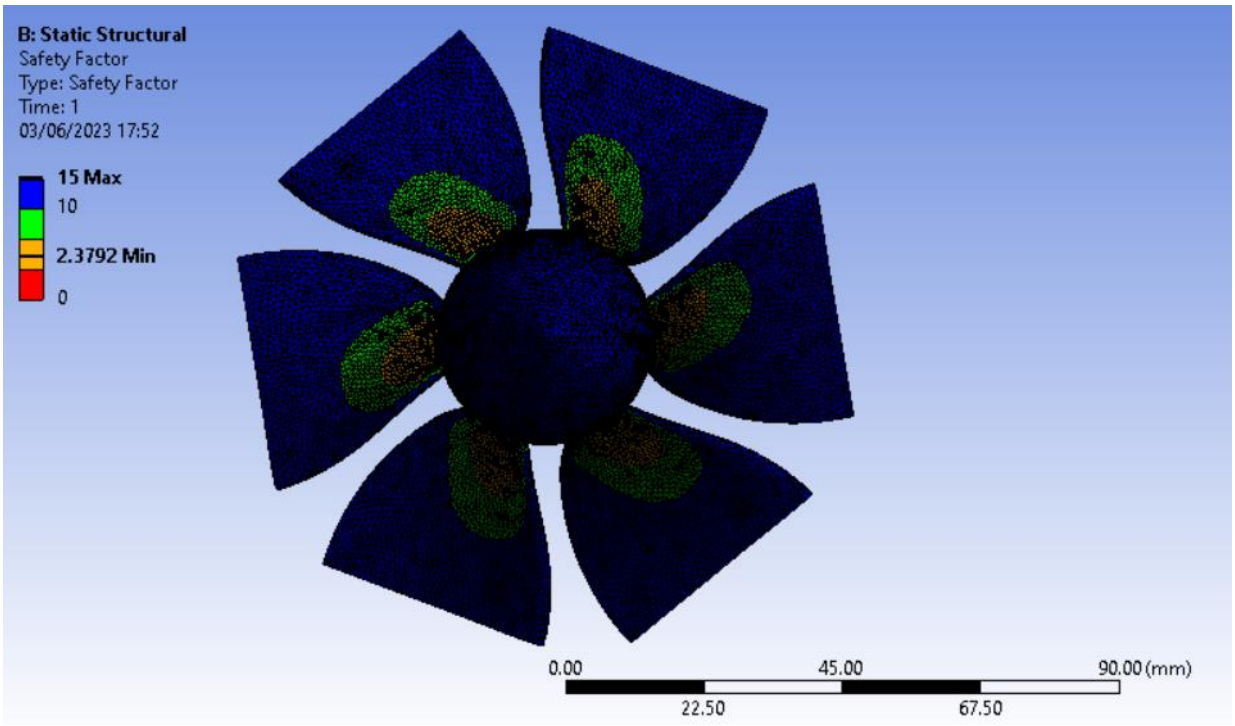

4.3.2 Banki Michell Turbine

Von Mises Contour

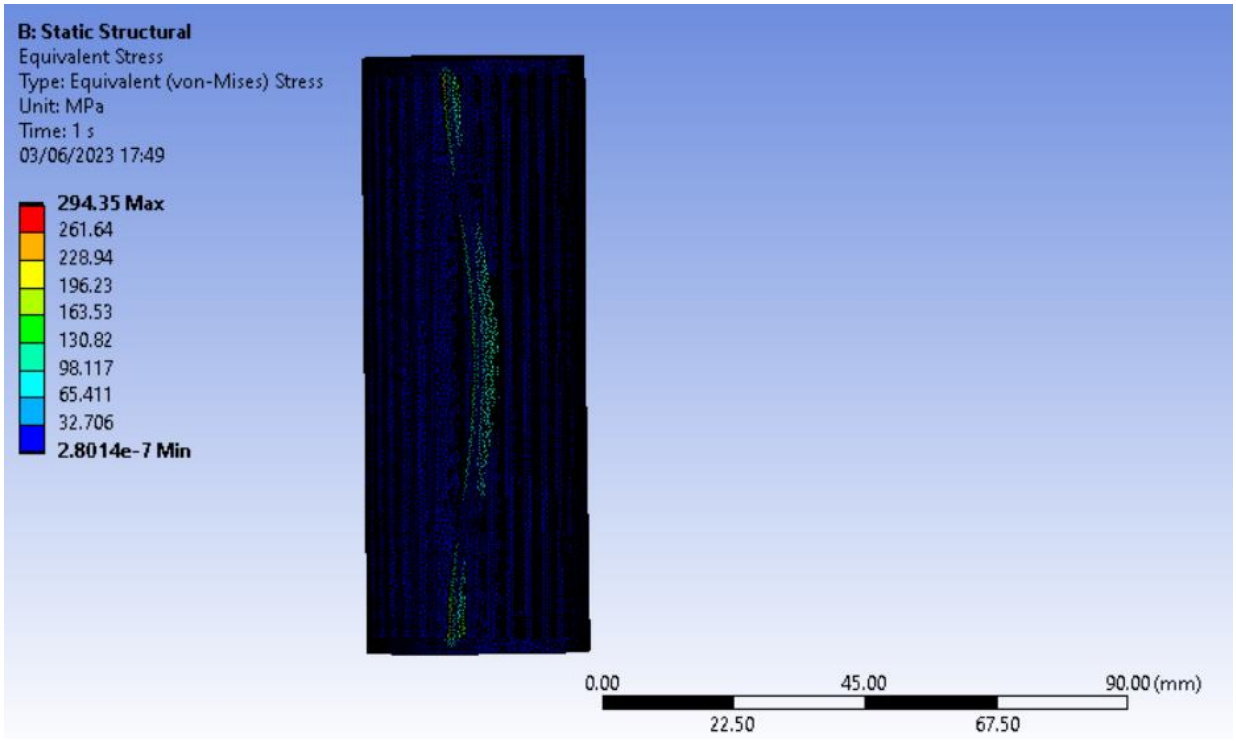

FOS Contour

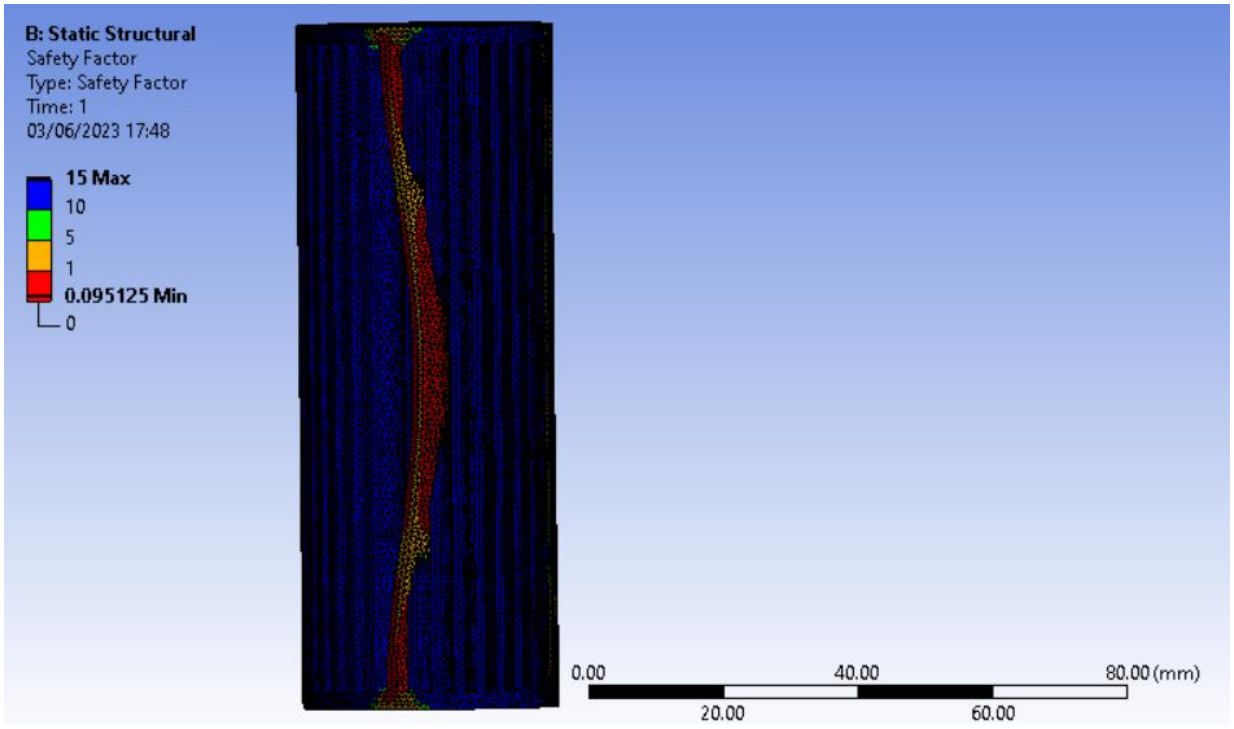

4.3.3 Darrieus Turbine

Von Mises Contour

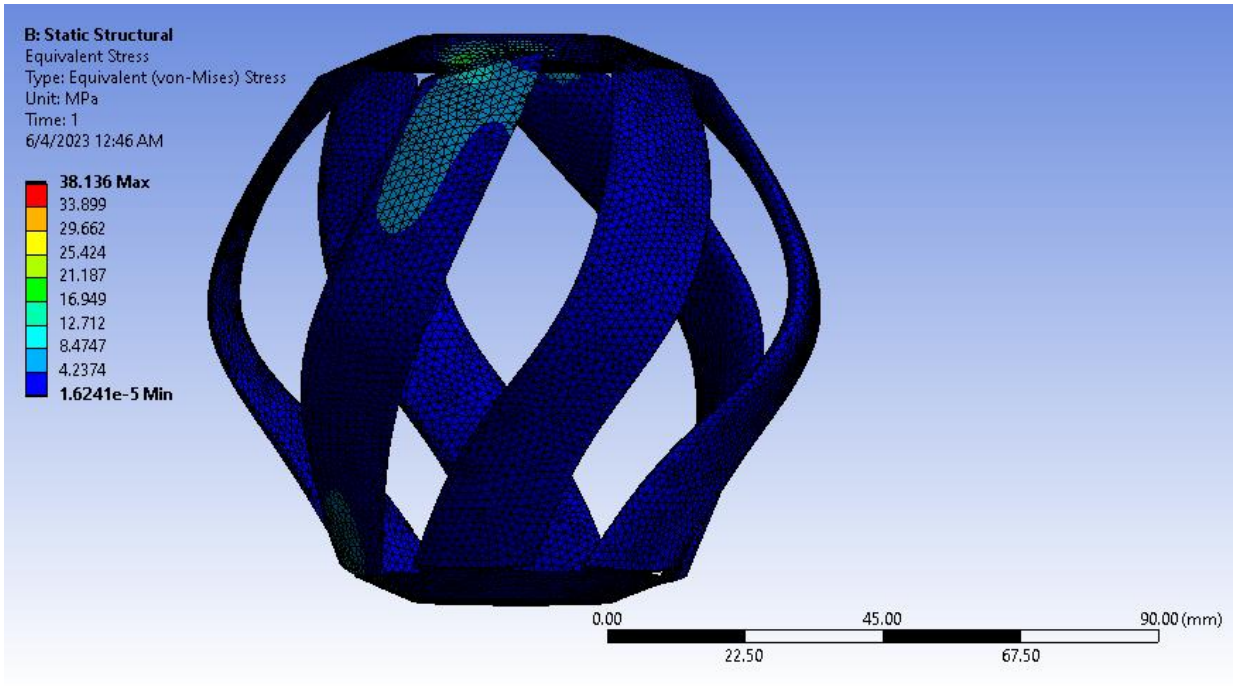

FOS Contour

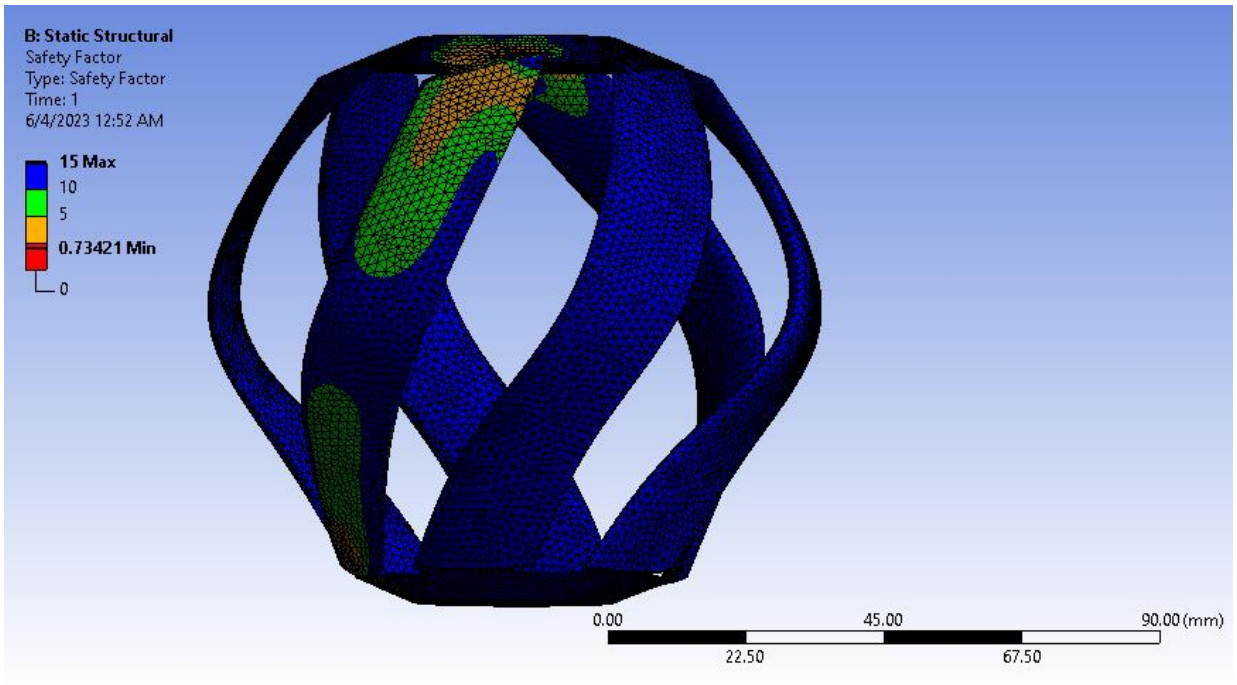

4.3.4 Savonius Turbine

Von Mises Contour

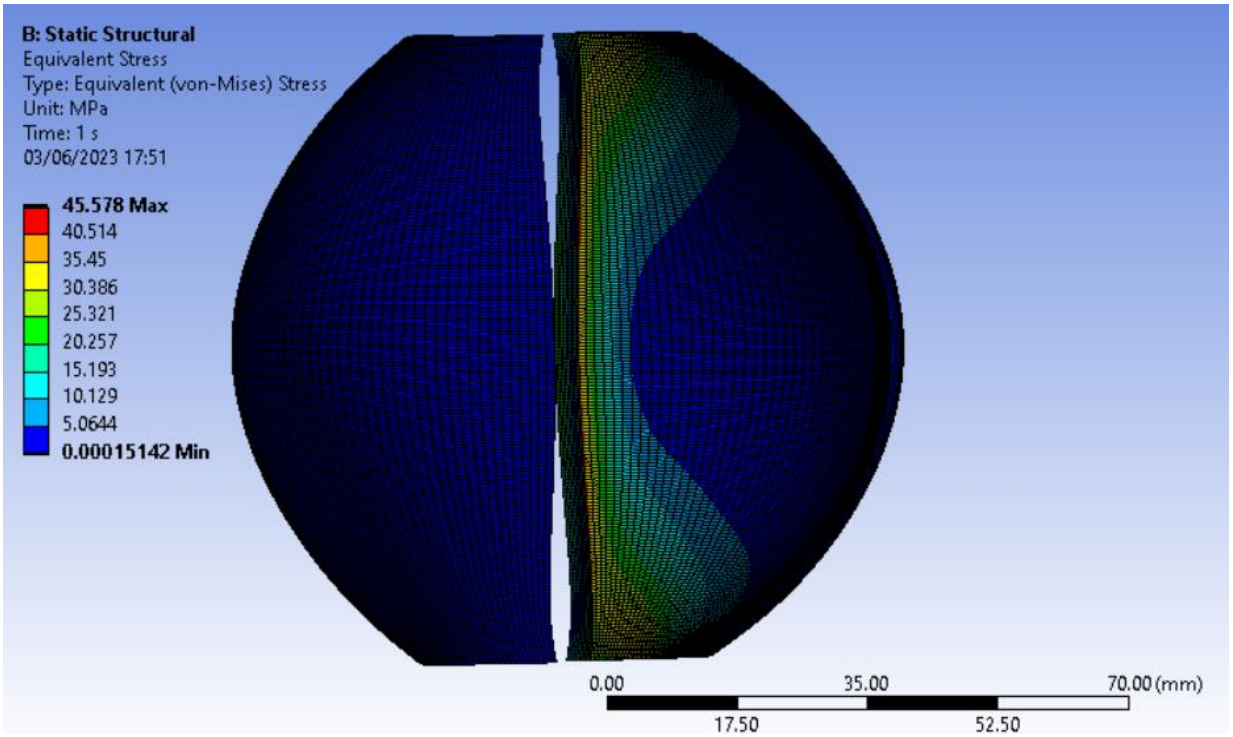

FOS Contour

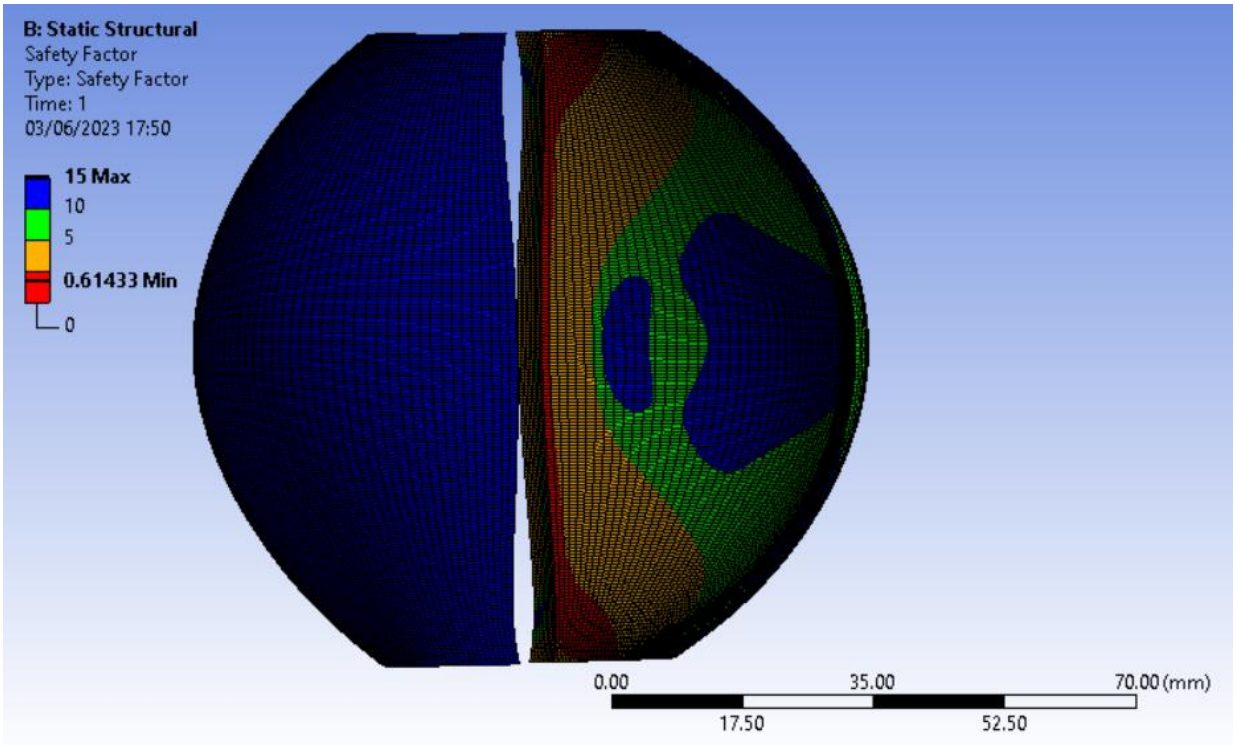

4.4 Von Mises Stress and FOS Comparison

Turbine	**Maximum Von Mises Stress (MPA)**	**Minimum Factor of Safety (FOS)**
Kaplan	11.769	2.3792
Michell Banki	294.35	0.095125
Darrieus	38.136	0.73421
Savonius	45.578	0.61433

It can be observed from the above table that under the design flowrate of 0.05735 m^3/s, the Kaplan turbine produces the least Von Mises Stress as well as the maximum factor of safety (FOS). Therefore, the Kaplan turbine was selected for fabrication.

FABRICATION

5.1 Overview

The selected Kaplan turbine was manufactured using 3D printing. Furthermore, the material used for manufacturing was chosen to be PETG which is a Glycol Modified version of Polyethylene Terephthalate (PET). Furthermore, PETG is a semi-rigid material with good impact resistance having a tensile yield strength of 50 MPa and an elastic modulus of 2.1 GPa. Four components were manufactured using 3D printing namely Kaplan turbine, Kaplan turbine shaft, mounting and in-pipe shaft support. Lastly, a suitable bearing and a DC motor was purchased from the local market which was used inversely as a generator.

5.2 Components

5.2.1 Kaplan Turbine

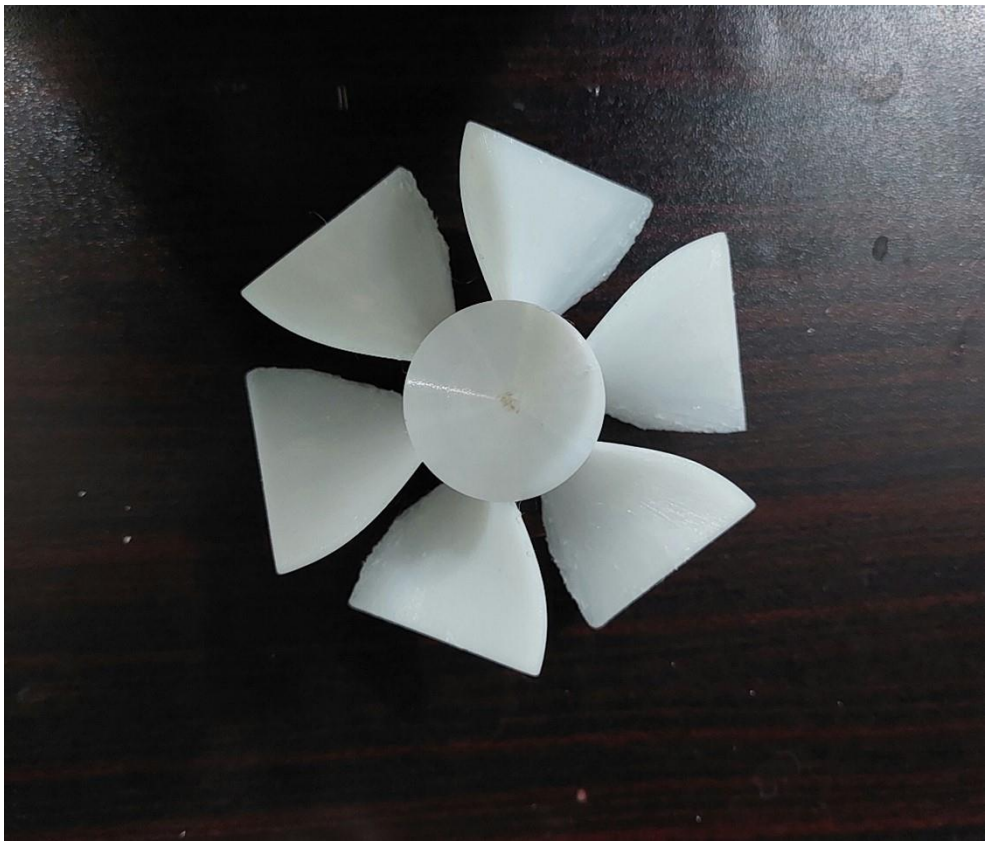

5.2.2 Kaplan Turbine Shaft

5.2.3 Mounting

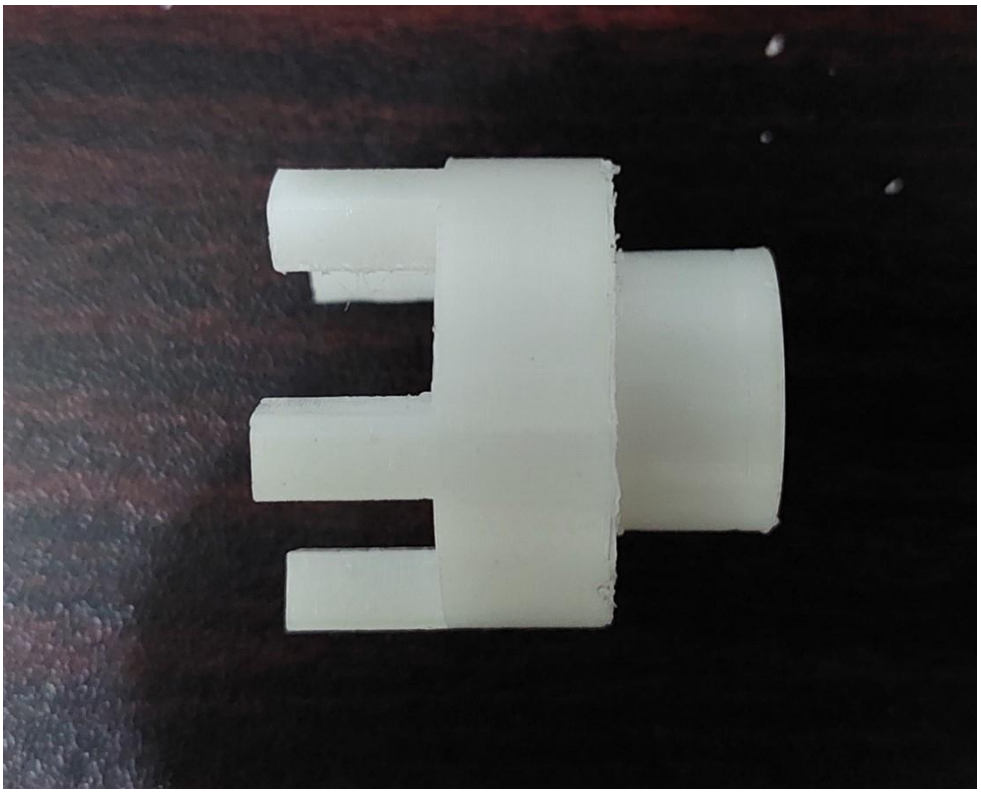

5.2.4 Shaft Support Stand

5.2.5 Bearing (ID = 30mm, OD = 42mm)

5.2.6 12V/3A DC Motor

5.3 Assembly

5.3.1 Schematic Diagram

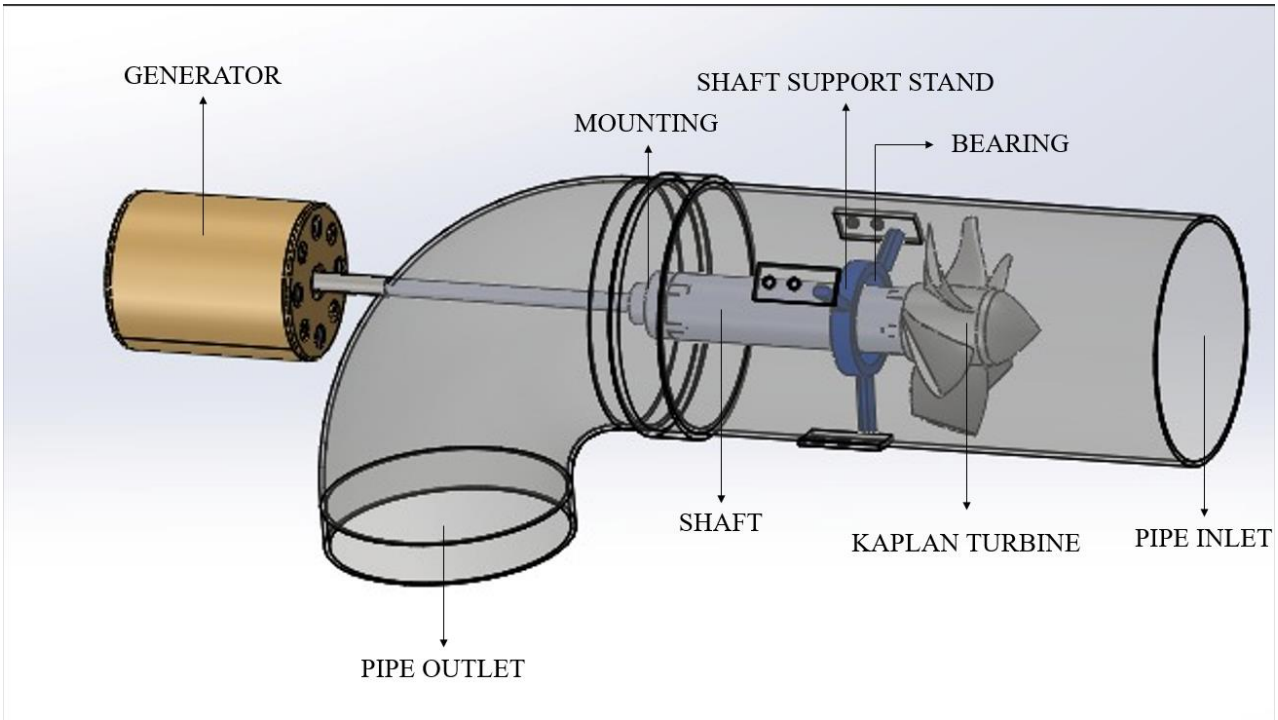

5.3.2 Prototype Model

EXPERIMENTAL ANALYSIS

6.1 Overview

To perform the experimental analysis of the Pico hydropower generation system, we utilized the hydraulic workbench which was present in the Fluid Mechanics – II lab in the Mechanical department. In order to set up the Pico hydropower generation system on the hydraulic workbench, an acrylic sheet was carved out with respect to its dimensions. This allowed us to firmly stabilize the Pico hydropower generation system within the hydraulic workbench in order to obtain accurate results. The Pico hydropower generation system was tested across various flowrates varying from 0.00080 m^3/s to 0.00160 m^3/s which was the range in which the hydraulic workbench operated. Also, this flowrate range was below our design flowrate which kept the experimental analysis on the Pico hydropower generation system within the safe limit. Furthermore, the parameters of interest across this flowrate range were the voltage (V), current (I), power output (P) which were calculated using digital multimeter (DMM). Also, the rotational speed (ω) was obtained with the help of a tachometer. Lastly, the flowrate with (Q_{After}) and without ($Q_{Orignal}$) the Pico hydropower generation system was also recorded in order to observe the flowrate losses due to it. Furthermore, after thorough research from online resources, we came to observe that small domestic appliances operating between 1V to 3V had resistances in the range of 27.5 Ω to 125 Ω which are presented in the following table.

Domestic Appliance	**Volts Requires (V)**	**Resistance (Ω)**
LED Flashlight	3.00	55
Battery-Powered Fan	2.50	125
Mini Electric Shaver	2.25	60
Electric Toothbrush	2.00	30
Battery-Powered Car	1.50	27.5

Therefore, after taking the average resistance of the above-mentioned domestic appliances, we obtain a value of around 60 Ω. Therefore, the performed experimental analysis was carried out across a 60 Ω resistor and the parameters of interest were noted.

6.2 Experimental Setup

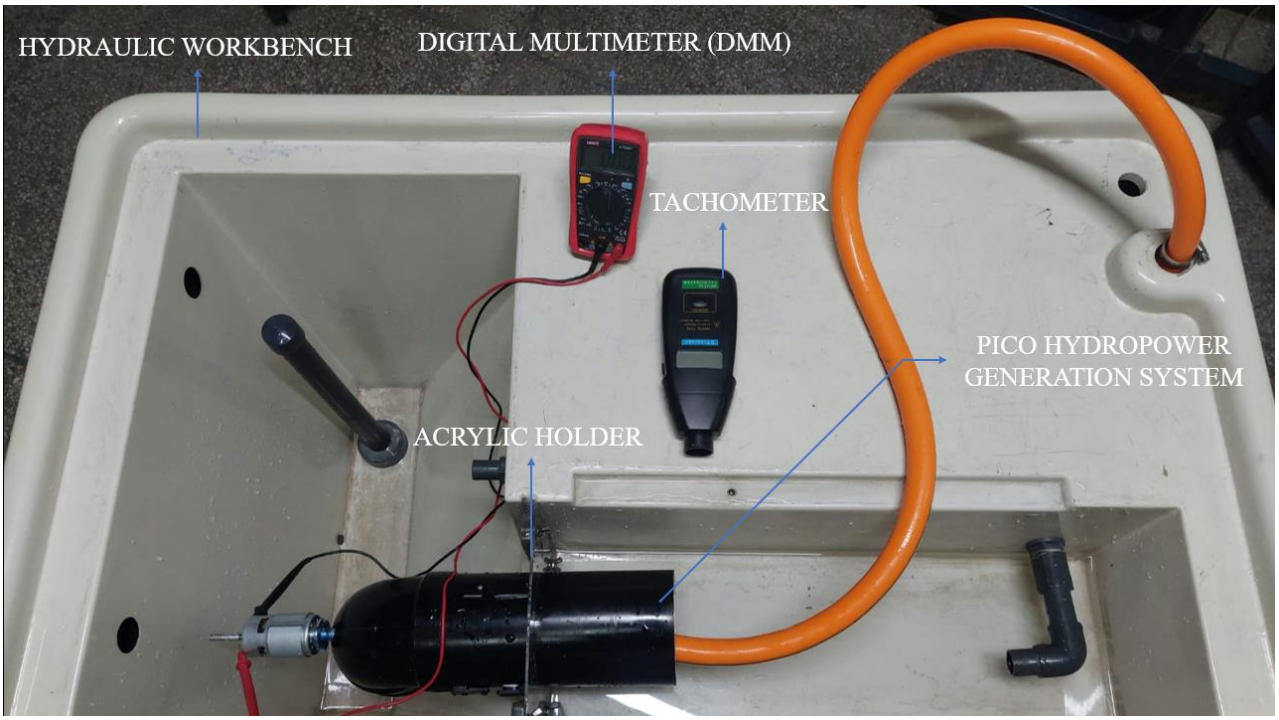

RESULTS

7.1 Experimental Readings

$Q_{Orignal}$ (m^3/s)	Q_{After} (m^3/s)	Voltage (V)	Resistance (Ω)	Current (mA)	Rotational Speed (RPM)
0.00160	0.00140	3.10	60	52	2100
0.00140	0.00123	2.34	60	39	1840
0.00120	0.00105	1.70	60	28	1460
0.00100	0.00088	1.30	60	22	1000

$Q_{Orignal}$ (m^3/s)	Q_{After} (m^3/s)	Power (Watt-hr)
0.00160	0.00140	580
0.00140	0.00123	329
0.00120	0.00105	171
0.00100	0.00088	103

7.2 Graphs

7.2.1 Voltage vs Flowrate

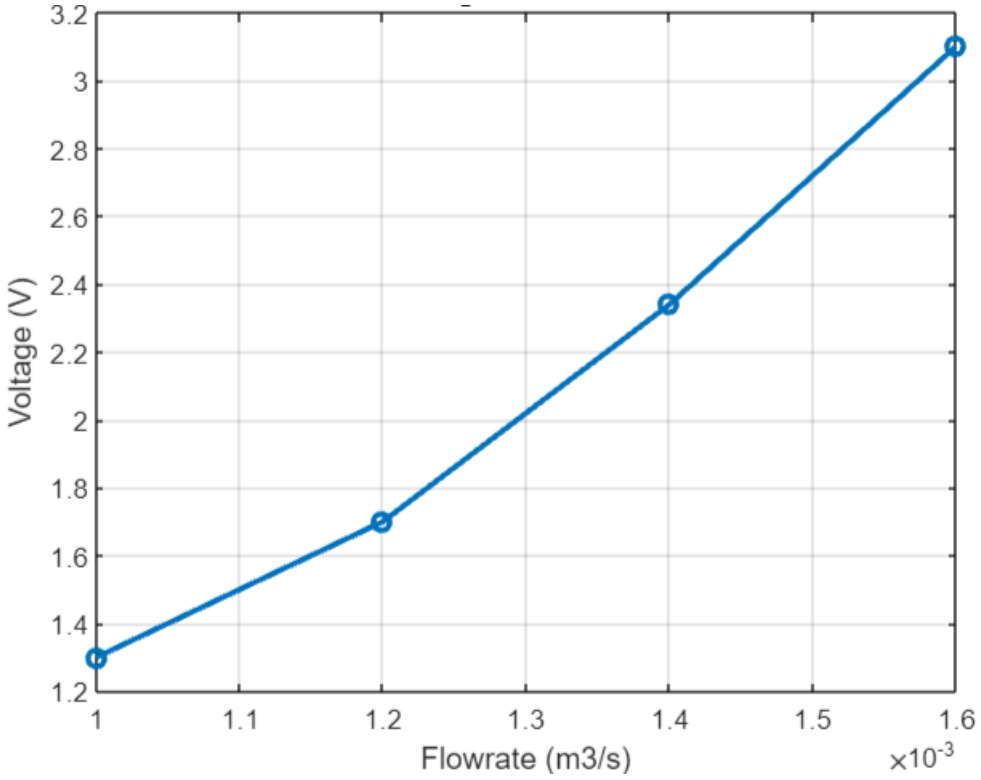

7.2.2 Current vs Flowrate

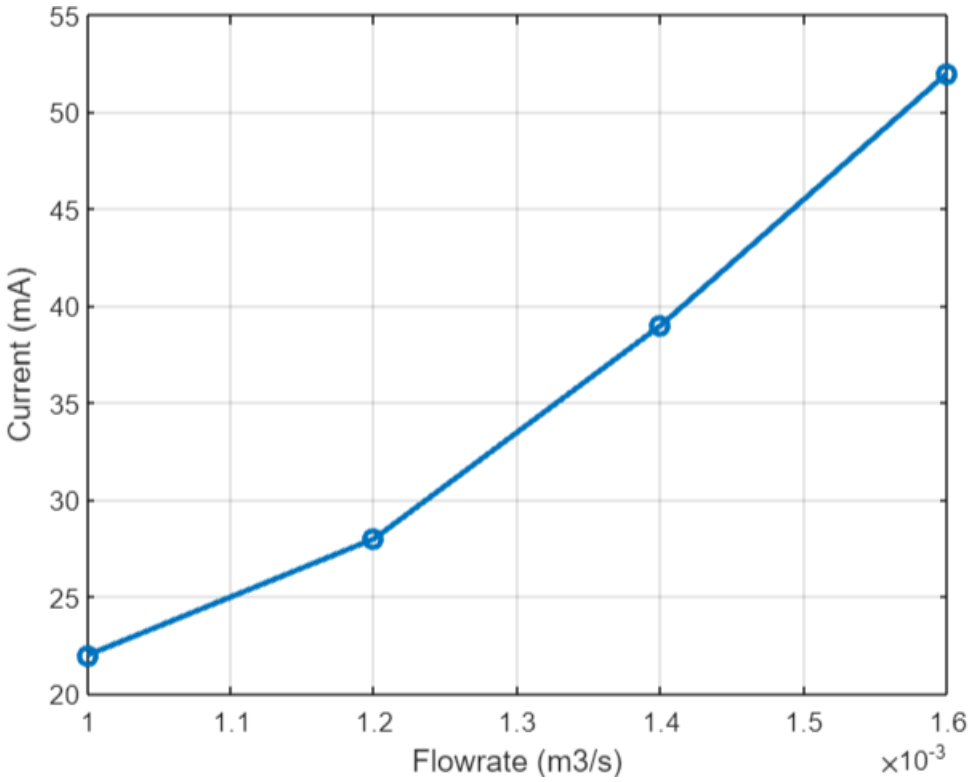

7.2.3 Rotational Speed vs Flowrate

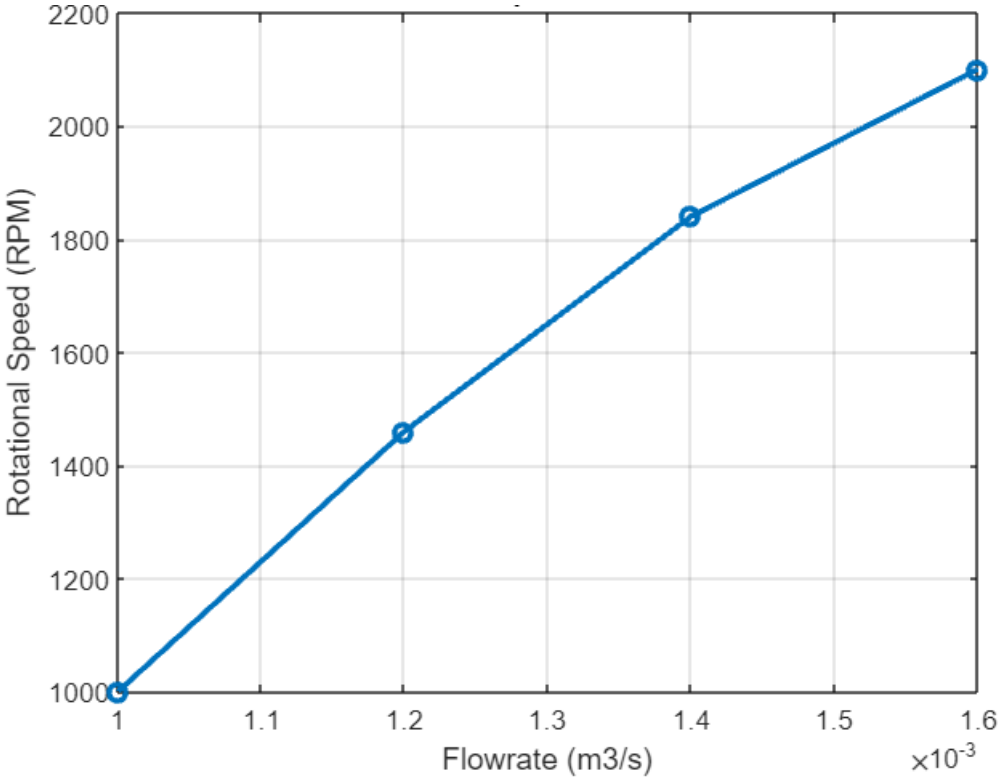

7.2.4 Power vs Flowrate

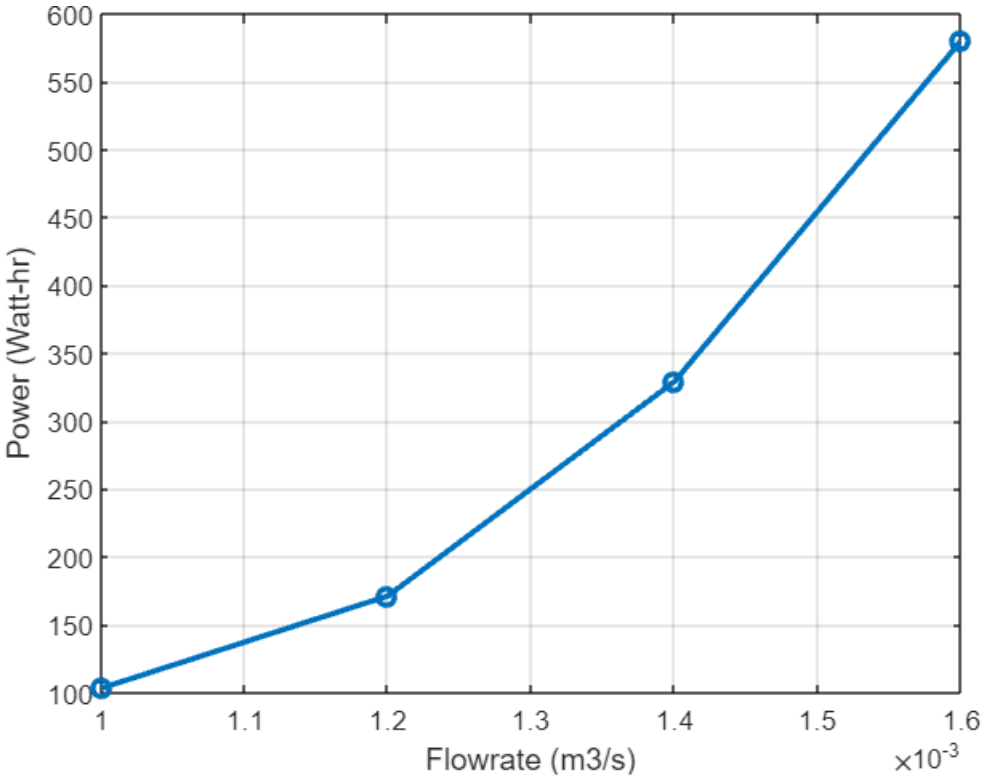

7.3 Discussion

Firstly, it can be observed that when the flowrate is varied from 0.00100 m^3/s to 0.00160 m^3/s across the 60 Ω resistor, the voltage varied from 1.30 V to 3.10 V. In addition, the current varied from 22 mA to 52 mA and the rotational speed varied from 1000 RPM to 2100 RPM. Consequentially, the power output varied from 103 Watt-hr to 580 Watt-hr. Although there was no linearity observed, the voltage, current, rotational speed and the power output increased when the flowrate was increased. Furthermore, another parameter was taken into consideration which was the payback period which determined the time period in which the Pico hydropower generation system would break even with its cost and become self-sustainable. The payback period analysis was done for both domestic as well as industrial applications as the cost of electricity was 13.080 PKR/KWh and 41.900 PKR/KWh respectively. Lastly, the total cost of our project was approximately 23,000 PKR. However, the total cost reduces to extremely low levels of 8000 PKR if the Pico hydropower generation system is fabricated in the correct manner without any errors and miscalculations.

Flowrate (m^3/s)	**Power (KWh)**	**Payback Period in Domestic Applications**	**Payback Period in Industrial Applications**
0.00160	0.580	1 Month & 14 Days	14 Days
0.00140	0.329	2 Months & 18 Days	25 Days
0.00120	0.171	4 Months & 29 Days	1 Month & 17 Days
0.00100	0.103	8 Months & 4 Days	2 Months & 17 Days

LIMITATIONS

8.1 Overview

Firstly, we have used a 12V/3A DC motor in reverse as a generator to generate electricity. By using this, we have limited the maximum instantaneous power output that can be produced to 36 W which will surely be increased when the flowrates approach the design flowrate of 0.05735 m^3/s. Secondly, the experimental analysis has been carried out in an extremely controlled environment. This is because we have tested the Pico hydropower generation system on the hydraulic workbench which possesses the ability to vary the flowrates from 0.00100 m^3/s to 0.00160 m^3/s but does not take the gross head into consideration which happens to be one of our design parameters. Furthermore, we took the non-conventional approach and fabricated the Pico hydropower generation system using 3D printing with the material as PETG which is a Glycol Modified version of Polyethylene Terephthalate (PET). This results in an increase in non-uniformity as well as an increase in surface roughness. Therefore, the shear stresses produced within the Pico hydropower generation system are also increased which leads to further power output losses.

RECOMMENDATIONS FOR FUTURE WORK

9.1 Overview

Firstly, in order to maximize the power output obtained, we recommend using a small dynamo instead of the 12V/3A DC motor used in reverse as a generator. This is because dynamo's are highly efficient, scalable as they are available in various dimensions, can be integrated into already existing power systems and provides rapid response when there is any fluctuation in the flowrate of water within the pipeline. Secondly, we recommend performing experimental analysis on the Pico hydropower generation system in applications which takes both the flowrate and the gross head into consideration such as high-rise residential buildings, university buildings, etc. This would provide much more accurate results and a better understanding of how the Pico hydropower generation system depends on the design parameters. Lastly, we recommend fabricating the Pico hydropower generation system using CNC machining and using Aluminum or Stainless Steel as the fabricating material. This would result in much more accurate dimensions of each individual component as well as a smooth surface finish which would reduce the overall power output losses and lead to an increase in the power output.

CONCLUSION

10.1 Overview

Firstly, this final year project has explored the significance of hydroelectric power generation systems as a sustainable and renewable energy source. As the world's population continues to grow and energy demand reaches its peak, the depletion of natural energy resources necessitates the exploration of new and innovative techniques to bridge the gap between energy demand and supply. Energy harvesting, in-pipe hydropower generation systems in particular, have emerged as a promising solution to meet these challenges.

In this project, we have primarily focused on Pico hydropower generation systems which can be utilized in high-rise residential buildings, water transmission pipelines as well water distribution networks to replace pressure regulation valves. This results in pressure regulation within the pipeline within the safe limit as well as clean and safe energy being harnessed from the potential and kinetic energy possessed by the water within the pipeline. Furthermore, we have studied the feasibility of four turbines namely the Kaplan, Banki Michell, Savonius and Darrieus turbines under our design parameters such as a design flowrate of 0.05735 m^3/s , gross head of 11 m and a pipe diameter of 0.1016 m. In addition, we performed ANSYS CFX and Static Structural analysis on each turbine individually under our design parameters. Von Mises Stress and factor of safety (FOS) were the two main parameters that were used to differentiate the performance of each turbines under the given conditions. After thorough analysis, the Kaplan turbine was manufactured and the Pico hydropower generation system was assembled. After performing experimental analysis, it was observed that the Pico hydropower generation system produced a minimum power output of 103 Watt-hr and a maximum power output of 580 Watt-hr corresponding to flowrates of 0.00100 m^3/s and 0.00160 m^3/s respectively. Also, when producing minimum power output, the Pico hydropower generation system had a domestic payback period of approximately 2 years and an industrial payback period of approximately 0.6 years. On the other hand, when producing maximum power output, the Pico hydropower generation system had a domestic payback period of approximately 0.35 years and an industrial payback period of approximately 0.1 years.

By conducting this project , we have shed light on the importance of in-pipe hydropower generation systems in addressing the growing energy demands while minimizing environmental impact. As the world strives for a more sustainable future, the findings of this project provide valuable insights for policymakers, energy planners, and researchers alike. Embracing and further developing in-pipe hydropower generation systems will contribute significantly to achieving a balanced and sustainable energy mix, fostering a greener and more resilient planet for future generations

REFERENCES

[1] https://www.sciencedirect.com/topics/engineering/energy-harvesting.

[2] https://www.usgs.gov/special-topics/water-science-school/science/hydroelectric-power-advantages-production-and-usage.

[3] https://www.enelgreenpower.com/learning-hub/renewable-energies/hydroelectric-energy/advantages.

[4] Casini, Marco. (2015). Harvesting energy from in-pipe hydro systems at urban and building scale. International Journal of Smart Grid and Clean Energy. 4. 10.12720/sgce.4.4.316-327.

[5] Jiyun Du, Hongxing Yang, Zhicheng Shen, Jian Chen, *Micro hydropower generation from water supply system in high rise buildings using pump as turbines*, Energy, Volume 137, 2017, Pages 431-440, ISSN 0360-5442, https://doi.org/10.1016/j.energy.2017.03.023.

[6] Prabir Sarkar, Bhaanuj Sharma, Ural Malik, *Energy generation from grey water in high raised buildings: The case of India*, Renewable Energy, Volume 69, 2014, Pages 284-289, ISSN 0960-1481, https://doi.org/10.1016/j.renene.2014.03.046.

[7] Youssef Itani, Mohamed Reda Soliman, Maher Kahil, *Recovering energy by hydro-turbines application in water transmission pipelines: A case study west of Saudi Arabia*, Energy, Volume 211, 2020, 118613, ISSN 0360-5442, https://doi.org/10.1016/j.energy.2020.118613.

[8] Christine Power, Aonghus McNabola, Paul Coughlan, *Development of an evaluation method for hydropower energy recovery in wastewater treatment plants: Case studies in Ireland and the UK*, Sustainable Energy Technologies and Assessments, Volume 7, 2014, Pages 166-177, ISSN 2213-1388, https://doi.org/10.1016/j.seta.2014.06.001.

[9] Gómez-Llanos, Eva, Juana Arias-Trujillo, Pablo Durán-Barroso, José M. Ceballos-Martínez, Jesús A. Torrecilla-Pinero, Carlos Urueña-Fernández, and Miguel Candel-Pérez. 2018. *"Hydropower Potential Assessment in Water Supply Systems" Proceedings* 2, no. 20: 1299. https://doi.org/10.3390/proceedings2201299

[10] Asmae Berrada, Zineb Bouhssine, Ameur Arechkik, *Optimisation and economic modeling of micro hydropower plant integrated in water distribution system, Journal of Cleaner Production*, Volume 232, 2019, Pages 877-887, ISSN 0959-6526, https://doi.org/10.1016/j.jclepro.2019.06.036.

[11] Ming Liu, Lei Tan, Shuliang Cao, *Theoretical model of energy performance prediction and BEP determination for centrifugal pump as turbine*, *Energy*, Volume 172, 2019, Pages 712-732, ISSN 0360 5442, https://doi.org/10.1016/j.energy.2019.01.162.

[12] Roland Uhunmwangho, Mathias Odje, Kenneth E. Okedu, *Comparative analysis of mini hydro turbines for Bumaji Stream, Boki, Cross River State, Nigeria*, Sustainable Energy Technologies and Assessments, Volume 27, 2018, Pages 102-108, ISSN 2213-1388, https://doi.org/10.1016/j.seta.2018.04.003.

[13] Teruhisa Kumano, Kotomi Matsunawa, Ryusuke Nishiyama, *Experimental Test and Feasibility Study of a Micro In-Pipe Hydropower Generator at a University Building*, IFAC-Papers Online, Volume 51, Issue 28, 2018, Pages 380-385, ISSN 2405-8963, https://doi.org/10.1016/j.ifacol.2018.11.732.

[14] T.L. Oladosu, O.A. Koya, *Numerical analysis of lift-based in-pipe turbine for predicting hydropower harnessing potential in selected water distribution networks for waterlines optimization*, Eng. Sci. Tech., Int. J. (2018), https://doi.org/10.1016/j.jestch.2018.05.016.

[15] Irene Samora, Vlad Hasmatuchi, Cécile Münch-Alligné, Mário J. Franca, Anton J. Schleiss, Helena M. Ramos, *Experimental characterization of a five blade tubular propeller turbine for pipe inline installation*, *Renewable Energy*, Volume 95, 2016, Pages 356-366, ISSN 0960-1481, https://doi.org/10.1016/j.renene.2016.04.023.

[16] Marco Sinagra, Costanza Aricò, Tullio Tucciarelli, Gabriele Morreale, *Experimental and numerical analysis of a backpressure Banki inline turbine for pressure regulation and energy production*, Renewable Energy, Volume 149, 2020, Pages 980-986, ISSN 0960-1481, https://doi.org/10.1016/j.renene.2019.10.076.

[17] Du Jiyun, Shen Zhicheng, Yang Hongxing, *Performance enhancement of an inline cross-flow hydro turbine for power supply to water leakage monitoring system*, Energy Procedia, Volume 145, 2018, Pages 363-367, ISSN 1876-6102, https://doi.org/10.1016/j.egypro.2018.04.065.

[18] https://theconstructor.org/practical-guide/kaplan-turbine-component-working/2904/.

[19] https://www.renewablesfirst.co.uk/hydropower/hydropower-learning-centre/kaplan-turbines/.

[20] https://www.sciencedirect.com/topics/engineering/kaplan-turbines.

[21] Sammartano, Vincenzo & Aricò, Costanza & Carravetta, Armando & Fecarotta, Oreste & Tucciarelli, T.. (2013). Banki-Michell Optimal Design by Computational Fluid Dynamics Testing and Hydrodynamic Analysis. Energies. 6. 10.3390/en6052362.

[22] A. J. Perez-Rodriguez, J. Sierra-Del Rio, L. F. Grisales-Noreña, S. Galvis, "Optimization of the Efficiency of a Michell–Banki Turbine Through the Variation of Its Geometrical Parameters Using a PSO Algorith," WSEAS Transactions on Applied and Theoretical Mechanics, vol. 16, pp. 37-46, 2021.

[23] K. Bheemalingeswara Reddy, Amit C. Bhosale, R.P. Saini, Performance parameters of lift-based vertical axis hydrokinetic turbines - A review, Ocean Engineering, Volume 266, Part 4, 2022, 113089, ISSN 0029-8018, https://doi.org/10.1016/j.oceaneng.2022.113089.

[24] Anuj Kumar, R.P. Saini, Performance parameters of Savonius type hydrokinetic turbine – A Review, Renewable and Sustainable Energy Reviews, Volume 64, 2016, Pages 289-310, ISSN 1364-0321, https://doi.org/10.1016/j.rser.2016.06.005.

[25] Abeykoon, C., & Hantsch, T. (2017). Design and Analysis of a Kaplan Turbine Runner Wheel. In *The 3rd World Congress on Mechanical, Chemical, and Material Engineering (MCM'17)* (pp. 1-16). [HTFF151].

[26] airfoiltools.com

[27] https://www.youtube.com/watch?v=ymjoQUIWcbk&list=PLEZ_oA6sA7CxfCTj0yxRPNr5lEY-GNVst&index=1.

[28] Emanuele Quaranta, Jean Pierre Perrier, Roberto Revelli, Optimal design process of cross-flow Banki turbines: Literature review and novel expeditious equations, Ocean Engineering, Volume 257, 2022, 111582, ISSN 0029-8018, https://doi.org/10.1016/j.oceaneng.2022.111582.

[29] Du Jiyun, Yang Hongxing, Shen Zhicheng, Guo Xiaodong, Development of an inline vertical cross-flow turbine for hydropower harvesting in urban water supply pipes, Renewable Energy, Volume 127, 2018, Pages 386-397, ISSN 0960-1481, https://doi.org/10.1016/j.renene.2018.04.070.

[30] K. Bheemalingeswara Reddy, Amit C. Bhosale, R.P. Saini, Performance parameters of lift-based vertical axis hydrokinetic turbines - A review, Ocean Engineering, Volume 266, Part 4, 2022, 113089, ISSN 0029-8018, https://doi.org/10.1016/j.oceaneng.2022.113089.

[31] S. Abdolkarim Payambarpour, Amir F. Najafi, Franco Magagnato, Investigation of deflector geometry and turbine aspect ratio effect on 3D modified in-pipe hydro Savonius turbine: Parametric study, Renewable Energy, Volume 148, 2020, Pages 44-59, ISSN 0960-1481, https://doi.org/10.1016/j.renene.2019.12.002.

[32] Ragheb, M. (2014) Optimal Rotor Tip Speed Ratio. http://mragheb.com/NPRE%20475%20Wind%20Power%20Systems/Optimal%20Rotor%20Tip%20Speed%20Ratio.pdf